RESEARCH
ENGINEERING
RESEARCH
ENGINEERING
RESEARCH
ENGINEERING
RESEARCH

Copy 1

Technical Information Center & Library
National Mine Health & Safety Academy
1301 Airport Road
Beaver, WV 25813-9426
(304) 256-3266

LIBRARY

ENGINEERING
RESEARCH
INSTITUTE

IOWA STATE
UNIVERSITY
AMES, IOWA

ENGINEERING
RESEARCH
ENGINEERING
RESEARCH

OFR
73-43

ENGINEERING RESEARCH

ENGINEERING RESEARCH
ENGINEERING RESEARCH
ENGINEERING RESEARCH
ENGINEERING RESEARCH

FINAL REPORT

PORTABLE BORE-HOLE SHEAR STRENGTH TESTER FOR COAL

R. L. Handy
D. E. Klockow
E. G. Ferguson

February 1973

Submitted to:

Technical Information Center & Library
National Mine Health & Safety Academy
1301 Airport Road
Beaver, WV 25813-9426
(304) 256-3266

ISU – ERI – AMES – 73037
ERI Project 909-S

ENGINEERING RESEARCH INSTITUTE
IOWA STATE UNIVERSITY AMES

Portable Bore-Hole Shear Strength Tester for Coal

FINAL REPORT

for the period

19 June 1971 - 15 August 1972

USDI - Bureau of Mines Grant G0101745 (MIN-46)

by

R. L. Handy,

D. E. Klockow,

and E. G. Ferguson

The contents contained herein were developed through the use of funds provided by the U.S. Department of the Interior, Bureau of Mines, and by this notice the Bureau does not agree or disagree with any of the ideas expressed or implied in this publication.

Iowa State University

Engineering Research Institute

Ames, Iowa 50010

LIST OF FIGURES

LIST OF TABLES

Portable Bore-Hole Shear Tester for Coal

SYNOPSIS

The objective of this research was to devise and test an apparatus to rapidly evaluate the cohesive and frictional strength of coal in situ, in order to increase the safety and percentage of coal recovery from underground coal mines.

During the first year a device was designed utilizing the bore-hole shear test principle from soil shear strength testing: Two opposing corrugated plates are forced outward to exert a controlled contact pressure against the sides of a previously bored hole, and then the plates are very slowly pulled along the axis of the hole to cause shearing of coal in contact with the plates.

Results with the device are expressed in terms of a friction angle ϕ and a cohesion c. The ϕ angles obtained from an Iowa coal are in close agreement with and fall between results from triaxial and direct shear laboratory tests on the same coal. The measured cohesion was found to be much less than from the comparable laboratory tests. It may be increased by pre-stressing and other techniques to embed the shear plate teeth for the first shear test point.

INTRODUCTION

Conventional coal mining involves removing portions of the coal and leaving other portions undisturbed to support the overlying layers of rock and soil. Thus coal is an engineering material, in that the portion remaining in walls and pillars must adequately support the overburden pressure. The objective of this research is to develop an in-situ strength tester for coal, in order to evaluate its supporting capacity and thereby increase the safety of mine operations while minimizing waste.

Coal is found in beds or seams which are either adjacent to or integrated with other deposited materials. During maturation of a coal seam, tectonic stresses develop which cause both macroscopic and microscopic cracks giving three planes of weakness: bedding or stratification planes, and cleats or fractures having two direction orientations normal to the bedding plane. These greatly influence strength.

REVIEW

Laboratory Strength Tests

The most elementary type of laboratory test to determine coal strength consists of shaping cubes of coal and subjecting them to a uniaxial loading condition (10)*. This is usually termed a crushing test; when the strength of the cube is exceeded, the cube is crushed. The stresses within the cube are not uniaxial but are three-dimensional or triaxial, due to the tendency of the cube to expand laterally when compressed axially under the applied load, while being restrained from lateral expansion by friction from

---

* Numbers in parentheses refer to the List of References appended to this report.

the loading platens. The actual stress state is therefore difficult to define, since it depends on end friction and on Poisson's ratio. The crushing test may be looked on as a model of coal behavior under similar loading geometry, for example to predict the strength of a coal column whose height equals its base dimensions. However, the axial load at failure has been found to vary with the size of the cube, larger cubes failing at lower unit stresses, probably due to the increasingly probability of encountering fracture defects as the specimen size increases. Empirical corrections based on tests of different sizes of cubes have been suggested, but strictly apply only to the coal tested.

Another simple laboratory test is the unconfined compressive strength test, where a cylinder or prism of material is uniaxially loaded to failure (19). This test differs from the crushing test by employing a sample where the height is greater than the width. If the height is much greater than the width (height to diameter ratio much greater than two), column action or bending affects the results, but when the height to diameter ratio is about two, the samples fail in shear or by axial splitting. The latter occurs when the loading platens offer little frictional resistance to both the top and bottom of the sample. Unconfined compressive strengths depend upon specimen size and shape, rate of loading, moisture content, and frictional behavior between platens and sample.

A common indirect shear test is the triaxial compression test (19). A cylindrical sample having a height-to-diameter ratio of about two is encased in a membrane and inserted into a pressure cell where an overall confining pressure is applied. During confinement, a uniaxial compressive stress is applied at the ends until the sample fails in shear. The triaxial test procedure is quite versatile in that any confining pressure can be selected and the uniaxial stress is applied independent of the confining stress.

Direct shear tests may be used to determine shearing strengths (15, 24), the basic types of shear tests being the single, double, punching, and torsional shear tests, or inducing direct shear under axial loading by using beveled dies to hold the sample. Each method employs a mathematical equation to convert shearing loads to shearing stresses. Brittle materials are not often tested by direct shear (19) because stress concentrations and combined shear and tensile stresses sometimes yield erroneous results.

Regardless of which laboratory test and procedure is used, considerable sample handling and shaping are necessary. Shaping brittle materials, either sawing or coring, employs water or air to flush cuttings and cool the cutting instrument. When coal is exposed to water, the fluid will readily migrate throughout the microfracture system because of high capillary tensions and may deteriorate strength between bedding planes. In addition to the influence of the microfracture system, larger cracks cause major sampling difficulties such that strengths resulting from laboratory tests do not adequately describe strengths in situ, in that only the stronger and more durable materials survive the sampling and preparation procedures.

In-Situ Strength Tests

The most common type of in situ strength test is the plate bearing test where a rigid geometrical area is forced against the rock body (1). Throughout the test, bearing stresses and bearing plate deformations are recorded until either the bearing stress decreases or remains constant for large plate penetrations. That maximum stress is termed the ultimate bearing capacity. The test is adaptable for coal or mine roof or floor material.

Penetration tests have also been conducted on coal (1). A round rod with either a flat, conical, or hemispherical head is forced into coal with a hydraulic apparatus to a pre-determined depth. In general, results showed resistance to penetration of as much as five times the unconfined compressive strength.

Attempts have been made to plow coal with a wedge-shaped cutting device (6). A bench is formed on the face of a coal column or wall and a wedge is forced through the coal at various depths. The plowing force is proportional to the coal unconfined compressive strength, the ratio of the plowing force to the unconfined compressive strength increasing with both depth of cut and with increasing blade angle. In addition, plowing forces for equal blade angles were found to be independent of the direction of plow with respect to cleat directions.

The modulus of rigidity, another material property, is defined as the shear stress divided by the shear strain, and is theoretically dependent upon Young's modulus and Poisson's ratio (17). A bore-hole testing device and procedure have been employed to determine the modulus of elasticity (sometimes termed the modulus of deformation) of rock in situ (21). With an assumed value for Poisson's ratio, usually 0.25 for rock materials, the modulus of rigidity, G, can be calculated. The test consists of inserting a cylindrical pressure cell into a bore hole and pumping a fluid into the cell. The volume of fluid pumped into the cell is related to the volume change of the drill hole and correlated with the applied pressure. Thick-walled cylinder equations for an elastic body are used to determine the elastic modulus. Calibrations are conducted at the site of the test to determine fluid compressibility and eliminate the need for a temperature correction.

Another test for determining rock deformability is the cable method (28). A cable is grouted into a vertical drill hole and used as an anchor for bearing stress applied through a steel beam to two adjacent concrete bearing blocks. Hydraulic jacks are used to force the beam off from the blocks, and the normal force on rock under the blocks is equal to one-half the tension in the cable. The normal stress and the penetration of the blocks into the rock are measured during the test.

In situ direct shear tests have also been conducted on mine rock. The method consists of carving a pedestal of rock, applying a dead weight surcharge to the top, and then shearing the pedestal at the base by applying a shearing stress horizontally with a hydraulic jack (27). While useful, they require large and unwieldly equipment.

OBJECTIVES

The purpose of this research was to design, construct, and test a portable borehole apparatus for determining the shearing strength of coal in situ. The following goals were established for this investigation:

1. The device must be mechanically simple, and sufficiently durable to withstand repeated use in adverse environmental conditions.

2. The unit itself, in addition to any necessary supplementary equipment, must be light in weight and easily transportable.

3. The operator must be able to employ a testing procedure with the apparatus positioned either horizontally, vertically, or at any angle.

4. Normal and shear stress capacities must be coincident with the high strengths encountered in rock bodies.

5. Time required to conduct a complete set of tests must be less than the time necessary to conduct a comparable set of tests using current laboratory and field methods.

6. Mechanisms of failure must be consistent with field occurrences and comparable to other testing procedures and theories.

In addition, at the end of the testing program, the investigators should make suggestions for improving the device and recommendations for further research.

FACTORS INFLUENCING SHEAR STRENGTH

Coal, like soil, is comprised of both solid volume and void volume. Individual particles, microscopic in size, have been tightly bonded together chemically during coal-forming processes. In 1773, Coulomb recognized the mechanisms of shear for granular materials as both friction and rupture behavior (5). He related friction to intergranular friction and particle interlocking, and rupture or cohesion to chemical bonding.

A simplified empirical method for describing rock shear strength is expressed by the Mohr-Coulomb equation, whereby strength relates to two parameters, cohesion and angle of internal friction. These shear strength parameters vary considerably with changes in environmental conditions. For example, moisture can influence rock strength in two ways (27), causing chemical and physical degradation of bonds between layers and individual particles, and in a saturated system reducing overall material strength (29) because portions of the applied stress are relieved from the mineral skeleton and carried by the pore fluid.

Very high confining stresses change rock structure by distorting individual grains or even fracturing individual particles. Normal particle interlocking and frictional characteristics therefore change, resulting in dependence of the friction angle on the confining pressure.

The shape of the Mohr envelope also is influenced by several variables which result from laboratory testing procedures (12, 27). Some of these variables are specimen size and shape, stiffness of the loading apparatus and the rate of loading, and platen friction.

A BORE-HOLE SHEAR COAL-TESTING DEVICE

Concept

The basic concept for a device to conduct direct shear tests along the walls of a hole bored in rock was adapted from the Iowa Bore-Hole Shear tester for soils (7, 11); where two corrugated plates are expanded at a selected constant pressure to engage material at the sides of the bore hole. The plates engaging wall material are then forced to move axially in the bore hole, causing the engaged material to be sheared.

Design of a Shear Head

The bore-hole shear instrument designed by the authors for coal testing is shown schematically in Figure 1. The larger cylinder housing the corrugated shear plates is about three inches in diameter, the approximate diameter of an NX bore hole in which the device is to be operated. One function of this cylinder is to transmit shear stresses from the material through the shear plates to the pulling rod.

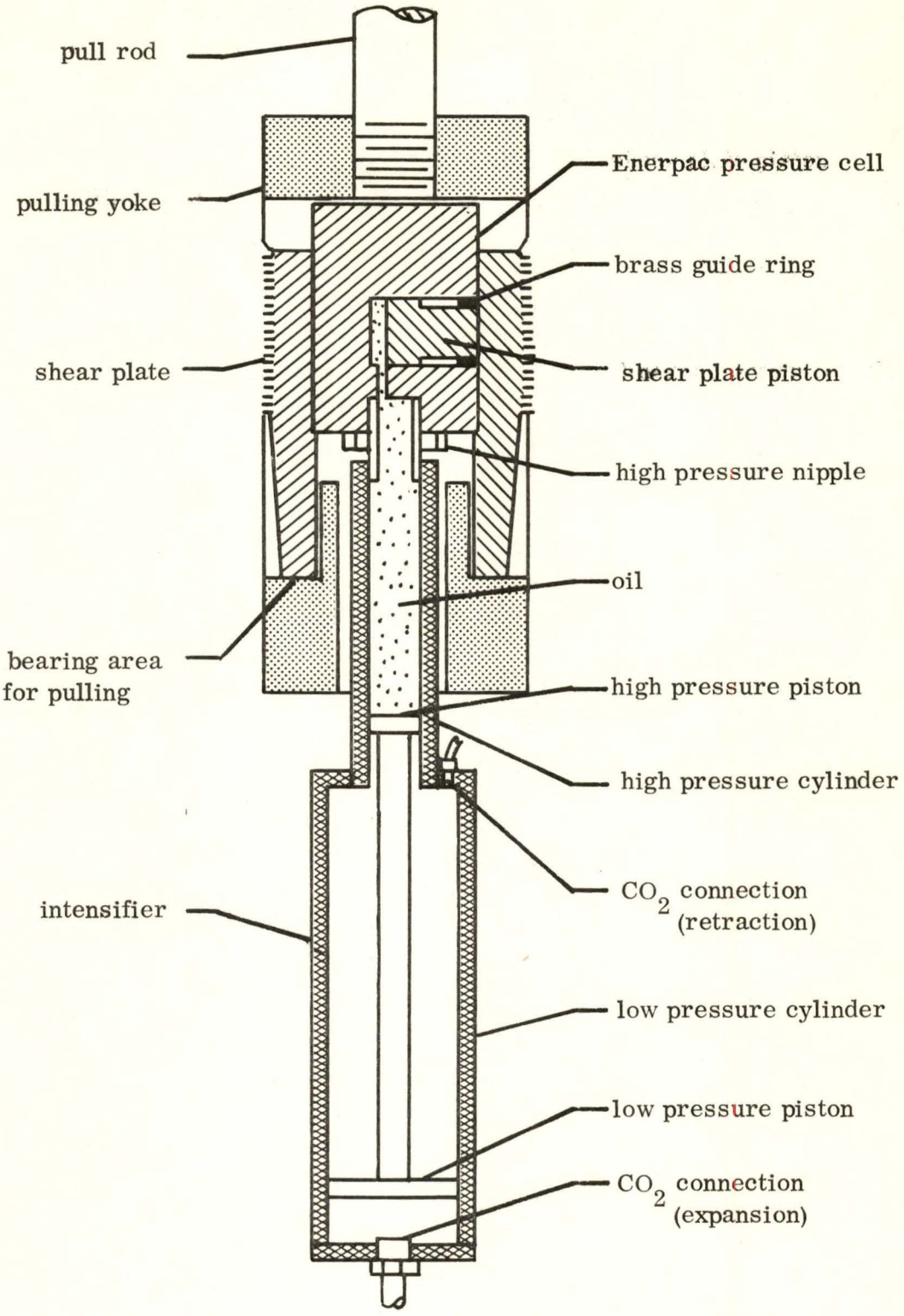

Figure 1. Section through expansion head assembly.

To expand the shear plates, pressurized carbon dioxide gas is fed to a 10:1 ratio pressure intensifier attached to the shear head. Hydraulic oil is used on the high pressure side to force the shear plates laterally by means of an Enerpac RC-50 hydraulic cylinder having a piston area of about 1 sq. in. No high pressure hydraulic lines are used. The maximum vapor pressure for carbon dioxide is 1040 psi at 86^{o}F, making the maximum oil pressure equal to 10,400 psi. The shear plates can be retracted by applying carbon dioxide gas pressure to the retraction port. The gross surface area of each shear plate is two square inches, resulting in a maximum normal contact pressure of about 5,000 psi. The CO_2 gas pressure is controlled by a pressure regulator and monitored by a 0-1000 psi pressure gauge. Calibrations were performed in a calibrated testing machine to allow conversion of gas pressures directly to plate contact pressures.

The entire expansion head assembly is heat-treated tool steel except for the high pressure cylinder which is stainless steel. To insure resistance to corrosion, all exterior faces were nickel plated.

Apparatus for Pulling

A photograph of the pulling unit is shown in Figure 2. Shear deformation, introduced by a worm and gear arrangement, is transferred to the shear head through a pulling rod threaded to fit the expansion head. The pulling rod has an external Acme-thread and a longitudinal keyway to prevent both the pulling rod and the expansion head from rotating during the test. The gearing of the pulling assembly is such that one turn of the crank applies about 0.001 inch of axial movement. The hydraulic cylinder holder and base plate fit loosely around the pulling rod and extend four inches into the bore hole so the unit

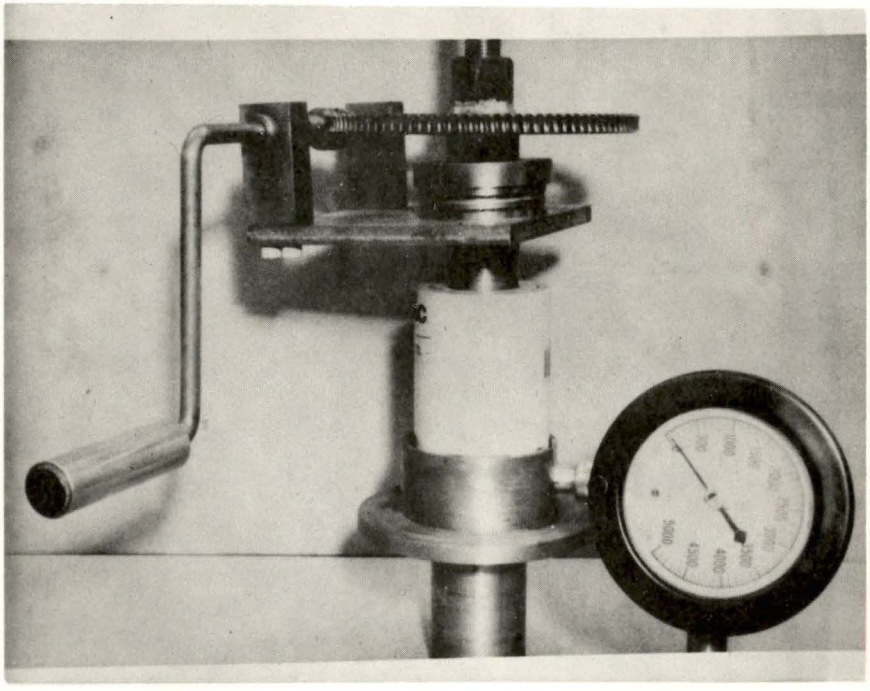

Figure 2. Pulling unit.

is self-supporting in a horizontal hole. A flange forms a base for pulling, and the larger end of this part is recessed to receive an Enerpac RC-20 40,000 lb. hydraulic cylinder fitted with a 10,000 psi pressure gauge to indicate shearing stresses. This cylinder has an axial hole for the pull rod, so pulling results in symmetrical loading.

Operation

The shear head is inserted into an NX bore hole and positioned at the desired depth, which is limited only by the amount of pull rod and pressure line available. The corrugated plates are expanded against the sides of the bore hole by gas pressure acting through the intensifier-hydraulic system. The expansion pressure relates to normal stress, σ, which is the independent variable of the Mohr-Coulomb equation. Shearing stress is induced by turning the hand crank, which pulls the rod and expanded shear head along the axis of the bore hole. Shearing deformation is continued until the shearing stress reaches a maximum and decreases. Normal stresses are relieved, the shear plates are retracted, and the expansion head is removed from the bore hole. The maximum shear stress, τ, obtained during the test is the dependent variable in the Mohr-Coulomb equation. The shear plate corrugations are cleaned, and the same procedure is repeated in untested coal in the same hole, using various normal stresses. Several such tests in one bore hole result in the Mohr-Coulomb failure envelope for the material being tested. The procedure just described is termed the conventional test procedure.

Another test procedure was developed and reverses part of the conventional test procedure: After each maximum shear stress has been attained for a given normal stress in the conventional test, the system is allowed to equilibrate. The shear stress decreases only slightly and remains at a value near the maximum attained during the

conventional test procedure. Because of the geometry of the apparatus, the shear stress may be held constant while the normal stress is decreased until slipping occurs and the shear stress abruptly decreases. The shear stress, τ, and the normal stress, σ, when the second type of shear occurs also are variables for the Mohr-Coulomb equation. As a result of the slip, the shear stress usually decreases and remains constant at some lower value, and the normal stress again can be decreased until a second slip occurs. The procedure is then repeated, such that several data points can be determined after each primary shear failure obtained by the conventional test procedure. This method is termed the relaxation test procedure and will be dealt with in a later section.

Comparative Laboratory Tests

As will be shown, the bore-hole shear test is extremely rapid compared to conventional laboratory shear tests. However, supplemental laboratory tests were required to obtain data for comparison with the bore-hole shear data. The supplemental tests used include a high-pressure triaxial method for 2 1/8 in. diameter by 4 in. high core samples, described in Appendix A, and a double-direct shear test on similar cores, described in Appendix B.

CONSIDERATIONS OF BORE-HOLE SHEAR FAILURE GEOMETRY

Direct shear tests consist of applying a normal stress to a sample and then applying sufficient shearing stress to cause the sample to fail. In general, the sample is constrained in two adjacent boxes or rings and is sheared as one part of the box or ring moves laterally with respect to the other half which is rigidly fixed. An inherent characteristics of this type of test is that the failure plane is fixed. In the bore-hole shear test the "sample" extends indefinitely away from the shear plates, and the position

of the failure plane is affected by other factors which are separately discussed in the following sections.

Criterion for Slip with Full Tooth Engagement

Figure 3 shows an idealized engagement of the inside of the bore hole by pre-cutting for the corrugations or teeth of the shear plates. To investigate the possibility of the teeth slipping on the contact surface prior to the material being sheared, an expression has been derived in Appendix C relating the force required to cause slipping to the normal force, the geometry of the interface, and the coefficient of friction for the mating surfaces. This expression is

$$F = N \tan (\theta + \varphi_\mu) \tag{1}$$

where: F is the shearing force,
N is the normal force,
θ is the bevel angle as shown in Figure 3, and
φ_μ is the angle of friction between the shear plate and the material ($\mu = \tan \varphi_\mu$).

Brown and Pomeroy (3) report the coefficient of sliding friction between coal and steel to vary with the sliding history. In addition, that coefficient is dependent upon the type of coal tested and increases with the distance moved. For steel-coal interfaces, the reported range for friction coefficients is from 0.44 to 0.83, giving φ_μ from 24 to 40 degrees.

The Mohr-Coulomb equation, $\tau = c + \sigma \tan \varphi$, is the expression for the shear strength of the material. Also derived in Appendix C is an expression combining slippage and shear. The expression is

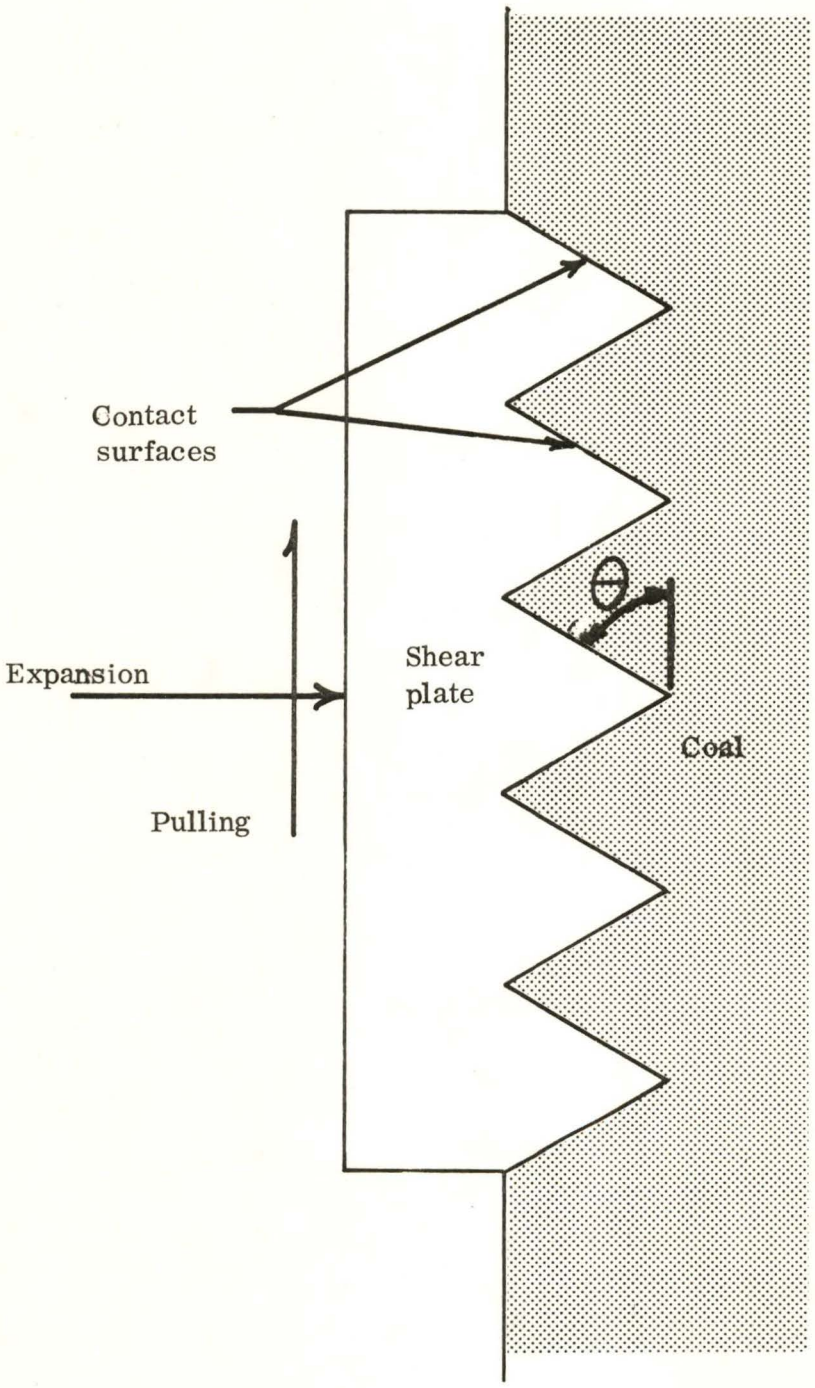

Figure 3. Idealized engagement of shear plate corrugations with tested material.

$$c/\sigma < \tan(\theta + \varphi_\mu) - \tan\varphi \qquad (2)$$

where: c = the material cohesion
σ = the normal stress applied to the material
φ = the material angle of internal friction, and
θ and φ_μ are as given above

Equation 2 expresses the condition for material shear instead of tooth slippage. The tooth geometry for the present bore-hole shear device fixes $\theta = 60^\circ$, giving for the lowest anticipated φ_μ of 24 degrees

$$c/\sigma < \tan(60 \pm 24) - \tan\varphi$$
$$< 9.5 - \tan\varphi$$

Using 60° for the highest anticipated φ for coal,

$$c/\sigma < 7.8$$

or $$c < 7.8\,\sigma$$

or $$\sigma < 0.13\,c$$

Thus for coal with $c = 1000$ psi, the minimum normal stress σ to cause material failure rather than slippage is 130 psi. As will be shown this is less than the friction which must be overcome for the apparatus to close, so slipping on the surface of the teeth is extremely unlikely.

It will be noted that $\tan(\theta + \varphi_\mu)$ becomes infinite as $(\theta + \varphi_\mu)$ approaches 90°. Thus with the lowest value for $\varphi_\mu = 24^\circ$, if $\theta = 90\text{-}24 = 66^\circ$ slipping will not occur regardless of the value of c. The 60° angle therefore appears to be a good choice for θ.

Tooth Engagement Without Pre-Cutting

While pre-cutting for tooth engagement was tried and still remains a possibility for future tests, major advantage can be realized by dispensing with this step -- that is, by expanding the shear head inside a smooth bored hole.

The corrugated shear plate shown in Figure 3 is a composite of several adjacent wedges. Stress distributions around wedges bearing into homogenous media are very complicated and nearly impossible to mathematically evaluate (9). Stresses, defined as load per unit area (30), are infinite as the wedge apex contacts the material because the area of a line is nonexistent. As the wedge further penetrates, the contact area as well as the normal stress reach some definable value. However, because no material can withstand infinite stresses, some fracture or failure has occurred. This localized failure stops when wedge penetration has provided a realistic cross sectional area for bearing. When consecutive wedges contact a material, such as with the bore-hole shear plate corrugations, brittle materials will partially fail in the region of the shear plate. Failure constitutes destroying cohesion and reducing the rock to granular material which would tend to fill between the corrugations.

After wedge penetration caused by application of the normal stress stops, a shearing stress is applied, tending to move the plates longitudinally in the bore hole. Movement causes material to be scraped from the sides of the bore hole and become tightly packed in the V-grooves. Additional longitudinal movement is accompanied by further shear plate penetration as shown in Fig. 4. Eventually all the corrugations are completely filled with tightly packed, pulverized material. Shearing then ideally could proceed across the asperities, aa' in Fig. 4, to give a valid measure of friction and cohesion, or it may follow the boundary between pulverized and unpulverized material, aba', or somewhere between. The development of Equation (2) is still applicable except that stresses will not be uniformly distributed. That is, there should be no sliding along the corrugation face, but the bearing area for the shearing stress is greatly reduced to ba'

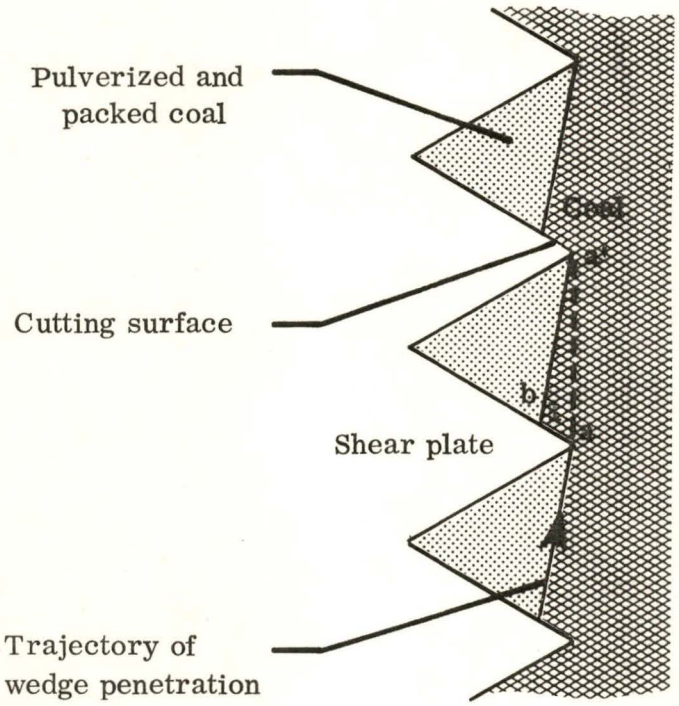

Figure 4. Penetration of the shear plate into smooth coal surface.

instead of the whole side of the corrugation, greatly increasing the plate-rock contact stresses. The distance ba' will depend on the cutting trajectory of the points, i.e. the relation between expansion distance and pulling distance, and is believed to be quite small. The high contact stresses, resulting elastic compression of coal in the neighborhood of the contact, and brittle nature of the coal all will tend to cause microfracturing ahead of the tooth.

After filling of the corrugations by densely packed, pulverized material, stress concentrations around the corrugation points will be relieved, and sliding will essentially be between densely packed pulverized coal and the unpulverized coal, giving a cohesion of zero and a friction angle which may be analogous to fractured or faulted coal.

Shear Plate Curvature

The above considerations were developed two-dimensionally. In the third dimension the contact plates must be curved to engage a portion of the circumference of the bore hole, Figure 5a. If the curvature of the shear plate does not match the curvature of the bore-hole circumference, a non-uniform stress distribution will result, as in Fig. 5b, c, and d. However, these non-uniformities will diminish as the teeth cut in, since cutting will be deepest at the locations of highest stresses.

A second factor is that circumferential friction, Fig. 5e, will reduce the effective normal stress. To minimize this effect the sector covered by the 1-inch-wide shear plate was made small, nominally $\frac{1}{3\ \pi} \times 360 = 38^{\circ}$. The maximum angular departure from the center of the plate is $38 \div 2 = 19^{\circ}$. At the edge of the plate a nominal 10 psi normal stress would be reduced to $10 \cos 19^{\circ} = 9.46$ psi, a maximum reduction of 5.4 percent due to circumferential friction. The average, obtained by integration, is 2.0 percent. Furthermore movement by the normally loaded shear plates along the axis of

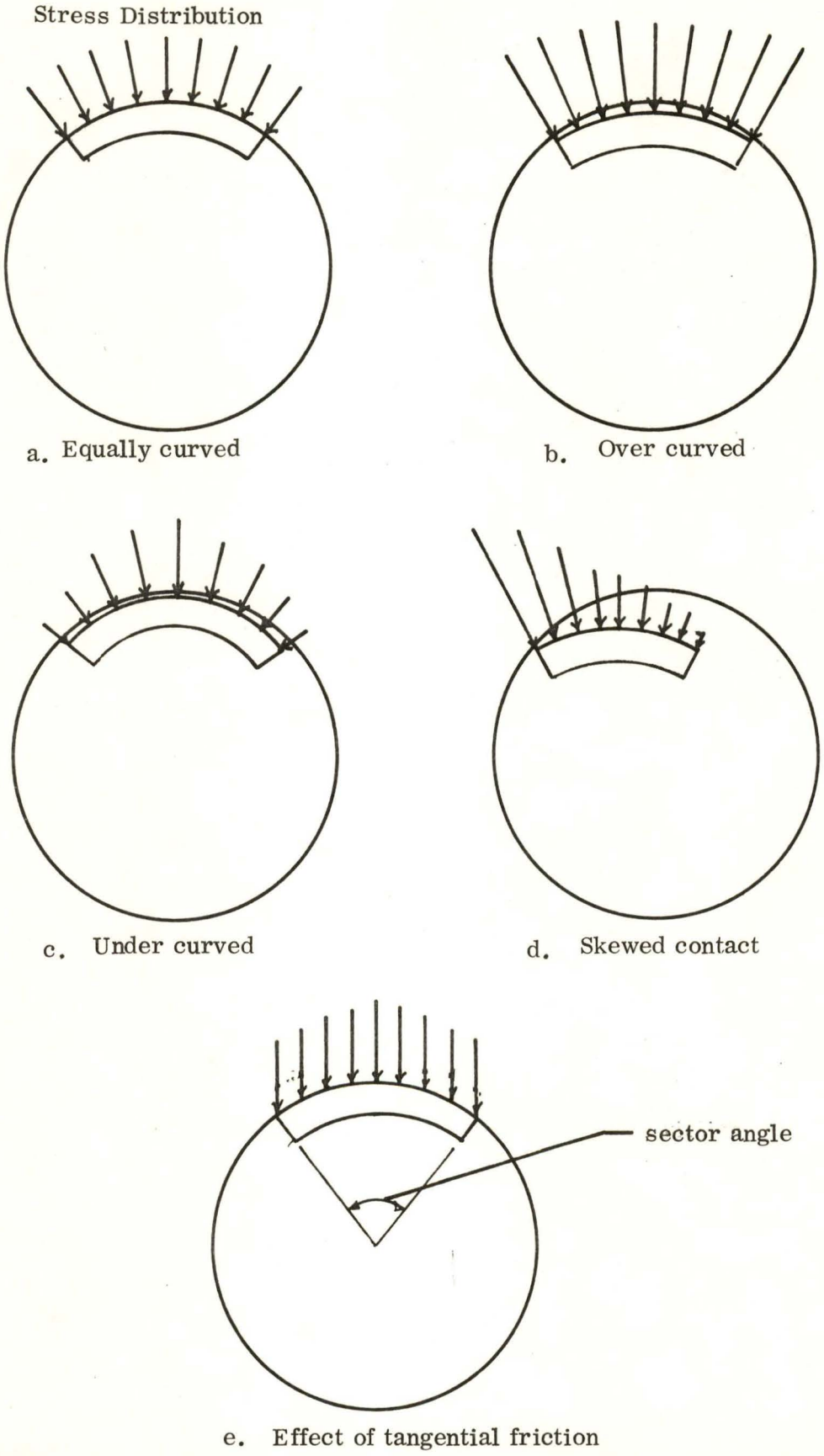

Figure 5. Circumferential fit of shear plate in the bore hole.

the hole will tend to relieve circumferential friction, so the reduction in normal stress due to circumferential friction is believed to be negligible.

Depth to Failure Surface

A previous investigation for the use of bore-hole shear devices in soil (11) showed on the basis of elastic theory (30) that shearing stresses decrease more rapidly than do normal stresses in the vicinity of plate loads, and thus failure should occur at the interface between the shear plate and the material tested. Although experimental work with a cohesionless sand and with plaster (Appendix E) shows the failure plane to occur away from the shear plate, shearing a brittle, cohesive material such as coal is anticipated to occur very close to the shear plate surfaces.

CALIBRATIONS

Expansion Calibration and Friction

The normal stress is monitored from the gas pressure gauge, and thus is affected by piston friction in the pressure intensifier and in the opening cylinder, and end friction on the shear plates. The latter is zero if no pulling stress is applied. Calibrations of the normal stress in psi versus gauge pressure with no pulling stress were found to be (Fifth Quarterly Report, p. 3):

$$\text{Conventional test (device opening):} \quad \sigma_c = 4.951\, P_\sigma - 52.39 \tag{3}$$

$$\text{Relaxation test (device closing):} \quad \sigma_c = 6.738\, P_\sigma - 99.60, \tag{4}$$

where P_σ represents the σ pressure gauge reading. Correlation coefficients for both relationships exceeded 0.999, indicating excellent linearity to pressure. The hysteresis is the difference, of $1.787\, P_\sigma - 47.21$, and represents twice the apparatus friction. Since the expression is for stress on a 2 sq. in. plate, the friction in pounds if friction during

opening is assumed to be equal to friction during closing is

$$F = 1.787\ P_{\sigma} - 47.21 \text{ lb.} \tag{5}$$

Thus for a pressure gauge reading of 600 psi, F is 1025 lb., and σ's from equations (3) and (4) are 2918 psi if the instrument is opening or 3943 psi if the instrument is closing. This friction and hysteresis are taken into account by the use of two calibration curves, one for opening and one for closing. If the instrument is neither opening or closing, as at the beginning of a relaxation test, neither calibration applies.

The second source of friction and hysteresis is end friction on the shear plates. A pushing arrangement was required because of the high stress levels required, but the plates were made long to encourage (Fig. 1) some rotation about the bearing areas. Whereas this end friction is independent of stress normal to the shear plates, it should vary with the shearing stress because of the steel-to-steel coefficient of sliding friction. This was evaluated from test data by performing both conventional and relaxation tests on essentially the same coal.* That is, since calibrations are used respectively for opening and closing, piston friction is accounted for, and the horizontal difference between τ vs. σ data plots for conventional and relaxation tests should be exclusively due to the plate end friction. Since such friction affects only σ, if φ_c and φ_r are the measured values of φ from the conventional and relaxation test, respectively, the φ value corrected for friction is (Appendix D):

$$\cot \varphi = \frac{1}{2} (\cot \varphi_c + \cot \varphi_r) \tag{6}$$

If the difference in φ_c and φ_r is small, relatively little error will result in using the numerical average to obtain φ:

---

*The following development based on test data differs from and is in lieu of hypotheses advanced in the Sixth Quarterly Report.

$$\varphi \approx \frac{1}{2}(\varphi_c + \varphi_r) \tag{7}$$

The analogous expression for cohesion is more complicated, and is derived in Appendix D.

Pulling Calibration and Friction

Similar to the normal stress calibrations, the shearing stress is applied by pulling against a sealed hydraulic cylinder during the conventional test, and acts oppositely in the relaxation test. Calibration curves obtained by use of a calibrated testing machine are (Fourth Quarterly Report, eq. 1 and Sixth Quarterly Report, eq. 5):

$$\tau_c = 1.205\ P_\tau - 43.471 \tag{8}$$

$$\tau_r = 1.183\ P_\tau - 122.6 \tag{9}$$

where τ is in psi and P_τ is the pressure gauge reading. Both correlation coefficients exceed 0.999. If the instrument is used in a vertical position the weight of the expansion head and pulling rod subtract from τ by an amount W/4 where W is the weight and 4 represents the shear plate bearing area in square inches.

Subtracting equations (9) from (8) gives the hysteresis, $0.022\ P_\tau + 79.3$, in terms of the effect on τ. Multiplying by the total shear plate area of 4 sq. in. gives $0.088\ P_\tau +$ 316 lb. If opening friction equals closing friction, dividing by two gives

$$F = 0.044\ P_\tau + 158 \text{ lb.} \tag{10}$$

Thus for a pressure gauge reading of 2000 psi, F is 88 + 158 = 246 lb, and τ's from equations (8) and (9) are 2366.5 psi or 2243.4 psi depending on whether the pulling force is increasing or decreasing. It will be noted that apparatus friction is considerably less than for the normal stress, there being no pressure intensifier. In addition the position of the pressure gauge in the pulling train is such that readings are not affected by the mechanical friction from gears, etc.

BORE-HOLE SHEAR TEST DATA FOR COAL

Initial Studies. Because of the difficulty in obtaining and curing uniform coal specimens, initial investigations were made utilizing plaster or neat cement to model coal. These tests were essential for "de-bugging" and understanding the apparatus and developing test procedures. Results are presented in Appendices E and F.

Preparation of Specimens for Tests. For convenience all coal tests were conducted in the laboratory. However, particular attention was paid that all apparatus and methods used would be readily adaptable to testing inside coal mines.

Two batches of coal were obtained from the Lovilia Coal Company, Lovilia, Iowa. Both quantities were treated as separate materials until shear strength results from each batch were obtained. Little strength difference was noted, and reported results include tests from both batches.

Figure 6 shows the first stage in sample preparation. Bulk chunks of coal were first cored with a 6-in. diameter diamond core barrel. The resulting cylinder was grouted with neat cement into a cylindrical, steel California Bearing Ratio (CBR) mold 6.00 in. inside diameter by 7.00 in. high.* This procedure allowed the coal sample to be tightly held for the second coring procedure and permitted handling without the risk of sample deterioration.

The second coring, performed with an NX core barrel three inches in outside diameter gave the desired bore hole plus a cylindrical core two and one-eighth-inches in diameter. The NX cores were later tested triaxially. Coring and testing were done both parallel and perpendicular to the bedding planes.

---

* ASTM Designation: D1883-67.

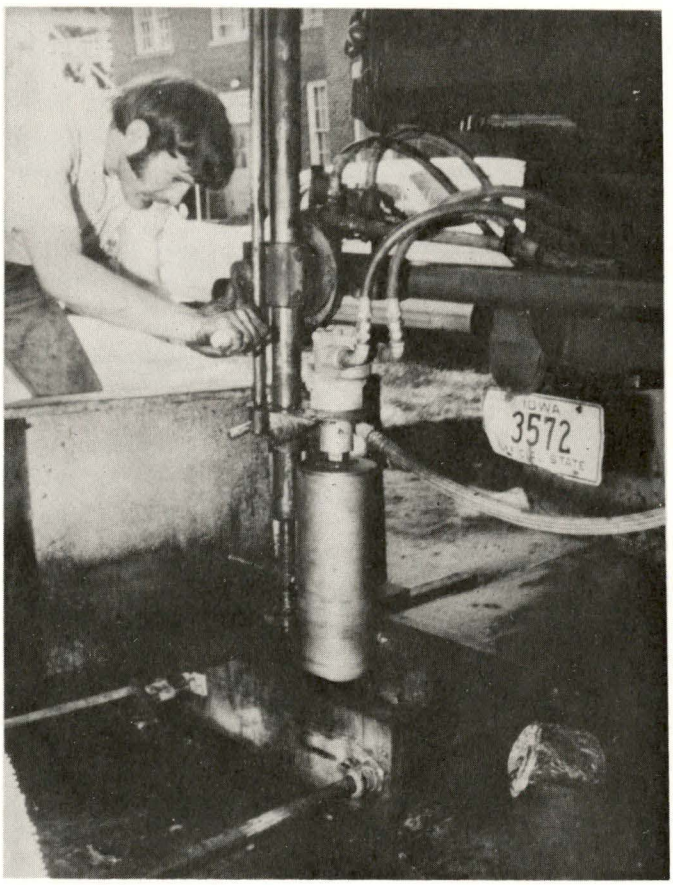

Figure 6. First stage in sample preparation for bore-hole shear tests on coal.

Results

Representative shearing stress vs. axial deformation curves are presented in Figure 7. In all cases the maximum shearing stress was selected as the failure stress.

A representative plot of failure shearing stresses vs. normal stresses for one test is shown in Figure 8. The slope of the curve is the friction angle φ; the intercept on the ordinate represents a cohesive strength, or extrapolated shearing strength with zero normal stress. Both conventional and relaxation test failure stresses are shown, converted from raw data by means of the appropriate calibration curves.

As previously discussed, the only apparatus friction not accounted for in calibration tests is that due to end bearing on the shear plates. This should subtract from the measured σ during conventional tests and add to it during relaxation: that is, plotted values of σ should be too high during the conventional test and too low during relaxation. Yet the regression lines fitted in Figure 8 practically overlap, and in fact would indicate a slight negative friction. The end bearing friction therefore appears to be negligible, suggesting that the shear plates either tilt instead of drag, or perhaps adjust during stick-slip, or cyclical relaxation of shearing stress on alternate plates due to non-symmetrical pulling during rotation of the drive gear.

One relaxation point in Fig. 8 at about 3500 psi calculated normal stress cannot be correct, since this normal stress is higher than that obtained for the preceding conventional test point, indicating that a full reversal of apparatus friction has not yet occurred, and neither calibration applies. This occurrence was rare and did not strongly influence the data reduction.

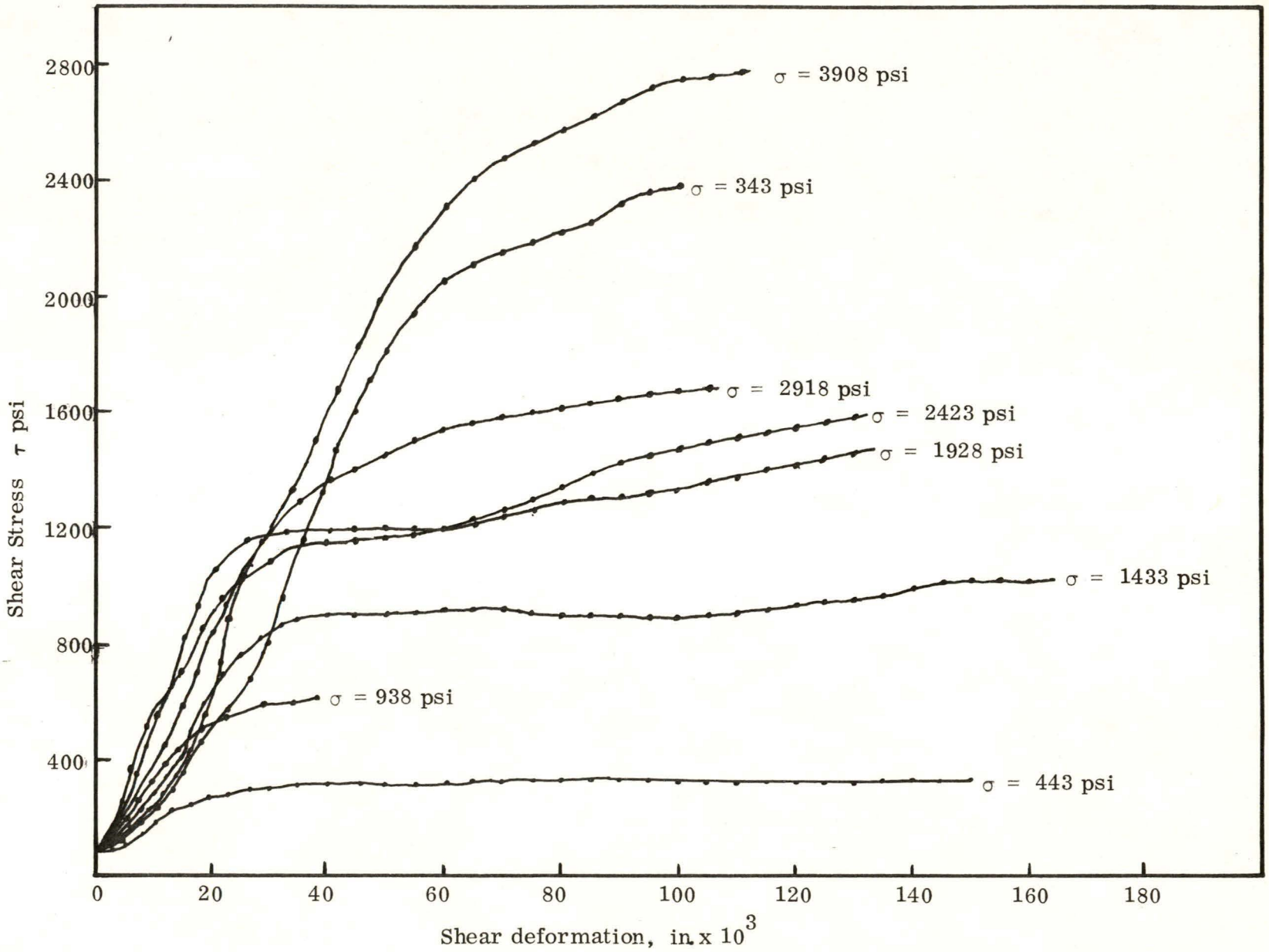

Figure 7. Stress-deformation curves for Test N, parallel to bedding planes.

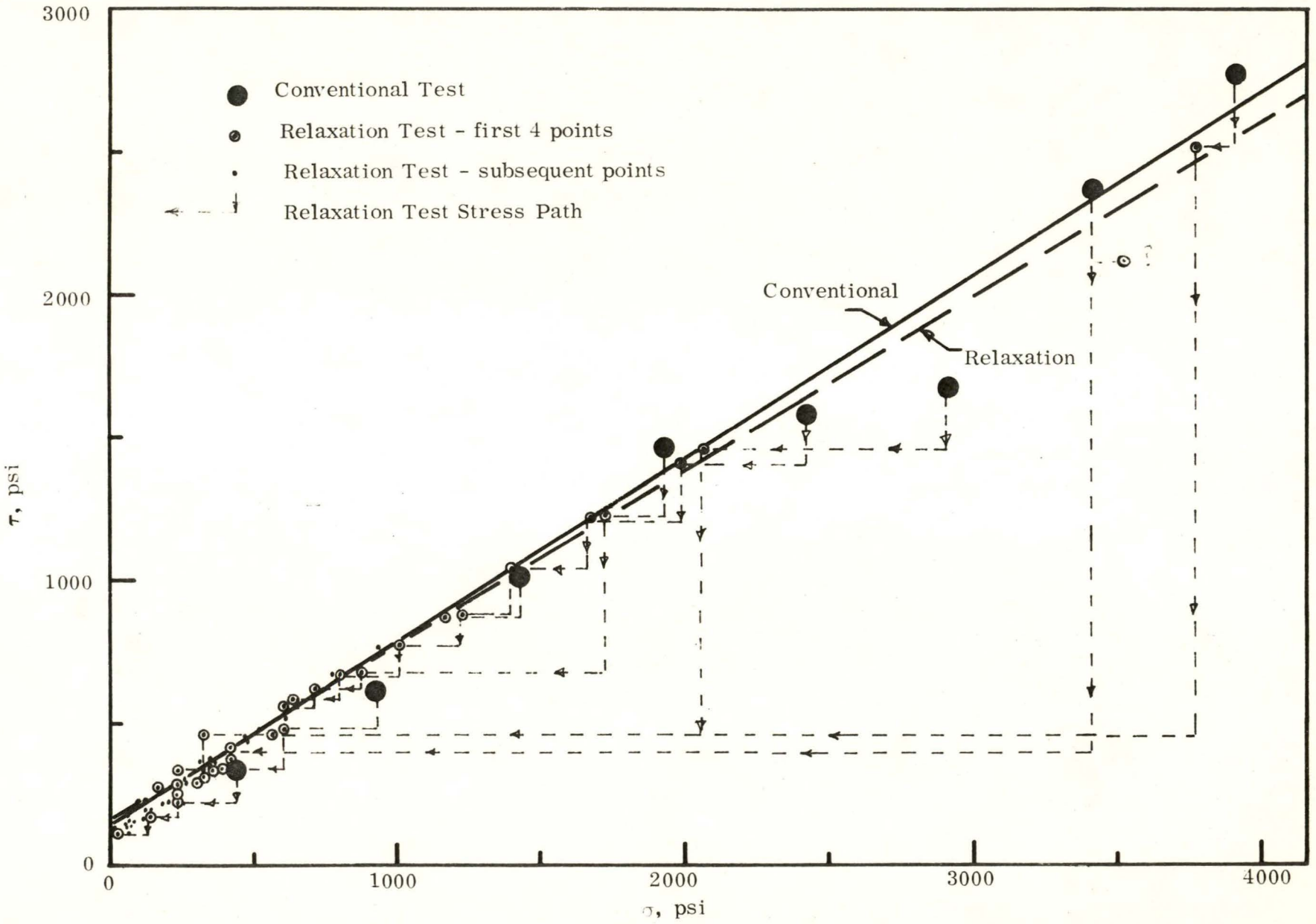

Figure 8. Results for Test N, parallel to bedding

In Fig. 8 can be seen that the relaxation test procedure gives many data points in the low stress range. To reduce needless duplication, ordinarily only the first four points obtained during each relaxation sequence were used in reduction of the data.

Strength with Shearing Parallel to Bedding Planes. Table I summarizes data from seven bore-hole shear tests conducted with shearing parallel to the bedding planes. In only three of the tests was φ_r greater than φ_c, and the average φ_r and φ_c differ only 0.77°, further indicating that shear plate end friction is negligible.

The standard deviation of the relaxation test φ_r is somewhat lower than that of the conventional test φ_c. Since the φ values are very close they may be shown to be of the same population, and additional confidence is gained from pooling the data, giving a mean φ or $\bar{\varphi} = 32.2 \pm 5.3^{\circ}$. The $\pm$ entry indicates 95% confidence limits on the mean, and includes sample variability.

The cohesions obtained by conventional and relaxation methods differ from each other and are much lower than typical for unaltered coal. It should be noted that pulverized and recompacted coal does have measureable cohesion, indicated by a tensile or flexural strength. This cohesion probably depends on the stress under which the material became packed. If this is true, the cohesion realized during the relaxation test should be somewhat higher than that from the conventional test, since the cohesiveness is inherited from a higher stress level. This is true for all but one test in Table I, and the average relaxation test cohesion is 143 psi, compared to an average of 22 psi from the conventional test. Cohesion may not develop until movement has been sufficient to fill the grooves and pressures are high enough to crush the reconsolidate the coal in the grooves. This would tend to give higher shear strengths at higher normal stresses, bending the failure envelope upward and giving higher values for φ_c and lower or negative values for c_c.

Table I

Bore-Hole Shear Test Results for Coal:

Shearing Parallel to Bedding*

Sample	Conventional Test				Relaxation Test			
	φ_c, °	c_c, psi	n	r	φ_r, °	c_c, psi	n	r
B	30.8	83.0	2	1.00	32.7	197.8	10	.979
C	37.8	-222.2	8	.997	32.9	174.6	26	.993
N	33.9	21.0	8	.985	31.5	145.8	31	.996
M	32.2	-43.0	5	.989	30.2	56.0	18	.971
O	33.5	48.0	7	.998	32.9	130.5	27	.995
P	32.4	140.5	4	.998	33.9	227.7	15	.993
R	27.8	128.4	4	.989	28.8	66.4	16	.966
Mean	32.6°	22.3 psi			31.9°	142.7 psi		
Std. dev.	3.05				1.78			
95% C.I.	± 7.5°				± 4.4°			

Mean φ from all parallel tests	32.2°
Standard deviation:	2.44
95% confidence interval:	±5.3°

* φ: friction angle; c: cohesion; n: number of data points; r: correlation coefficient.

Strength with Shearing Perpendicular to Bedding Planes. Table II presents data from eight bore-hole shear tests conducted with shearing across the bedding planes. Again the mean φ angles from the two types of tests are close, differing by 3.4^{o}, but the standard deviation and hence the confidence interval from the relaxation test is much greater than from other tests. Pooling the data therefore reduced the confidence in the mean, and the best mean was from the conventional test, where $\bar{\varphi} = 31.5 \pm 4.1^{o}$, the $\pm$ entry signifying 95% confidence limits on the mean.

Pooling the conventional test data from Tables I and II gives $\bar{\varphi} = 32.0 \pm 5.2^{o}$ for shearing either parallel or perpendicular to the bedding planes.

Results from Comparative Laboratory Tests

Direct Shear. Direct shear test results for one-inch diameter cores taken parallel and perpendicular to the bedding planes are shown in Figure 9 and Table III. The method and equipment used are described in Appendix B. Coal strength parameters for the direction of shear parallel to the bedding planes were $\bar{\varphi} = 31.6^{o}$ and $\bar{c} = 1611$ psi for the mean angle of internal friction and mean cohesion, respectively. The 95% confidence limits on $\bar{\varphi}$ are 21.4 to 40.0^{o}, a range of 18.6^{o}.* For the direction of shear perpendicular to the bedding planes, $\bar{\varphi} = 29.1^{o}$ with comparable precision, and $\bar{c} = 2151$ psi. Averaging the two data sets gives $\bar{\varphi} = 30.4^{o}$ and $\bar{c} = 1881$ psi. Thus the double direct shear test mean φ angles are closely comparable to those obtained by bore-hole shear, but with somewhat less precision, perhaps because of the influence of variable cohesion and micro-fracturing in the double direct shear test. The cross-sectional area sheared is also smaller in the latter test, nominally 1.57 sq. in. compared to 4.0 sq. in. in the bore-hole shear tests.

---

* Confidence limits on $\bar{\varphi}$ from direct shear and triaxial shear tests are actually on $\tan \varphi$ and $\sin \varphi$, respectively, and therefore cannot be given a symmetrical $\pm$ notation.

Table II

Bore-Hole Shear Test Results for Coal:

Shearing Perpendicular to Bedding*

Sample	Conventional Test				Relaxation Test			
	φ_c, °	c_c, psi	n	r	φ_r, °	c_r, psi	n	r
D	31.3	-183.9	3	.998	23.9	231.1	16	.956
E	28.0	32.7	4	.999	27.8	137.0	14	.994
F	33.4	39.3	4	.999	37.0	132.9	14	.972
L	32.4	86.5	8	.992	35.7	121.1	27	.990
V	33.1	74.9	4	.996	35.6	142.6	16	.996
W	31.1	181.4	4	.995	37.5	128.4	16	.993
X	30.4	78.8	4	.996	35.4	150.0	15	.978
Y	32.4	73.4	3	1.000	46.6	72.6	12	.974
Mean	31.5	47.9			34.9	139.5		
Std. dev.	1.73				6.77			
95% CI	$\pm$ 4.1°				$\pm$ 16.0°			

Mean φ from all perpendicular tests	33.2°	From all tests	32.0°
Standard deviation:	5.09		2.42
95% Confidence Interval:	$\pm$ 10.8°		$\pm$ 5.2°

* φ: friction angle; c: cohesion; n: number of data points; r: correlation coefficient.

Table III

Double Direct Shear Data on 1-in. Coal Cores

	Shear Direction to Bedding		
σ, psi	Parallel τ, psi	Perpendicular τ, psi	
163	2170	2248	
369	1104	2144	
576	2514	2468	
783	1897	1884	
989	1656	2533	
1196	2387	3612	
1402	2969	3183	
1609	2404	2962	
1815	2780	3261	
2022	2943	3677	
2229	3358	3638	
2435	2598	3196	
2642	3579	3872	
2848	3342	4028	
3055	3495	3118	
3261	3469	3846	
			All data:
φ:	31.6°	29.1°	30.4°
95% C.I. on φ:	$21.4 - 40.0^\circ$	$18.3 - 38.1^\circ$	$22.6 - 37.1^\circ$
c	1611 psi	2151 psi	1881 psi
c from $\sigma = 0$ tests	535 ± 124 psi	1520 ± 326 psi	

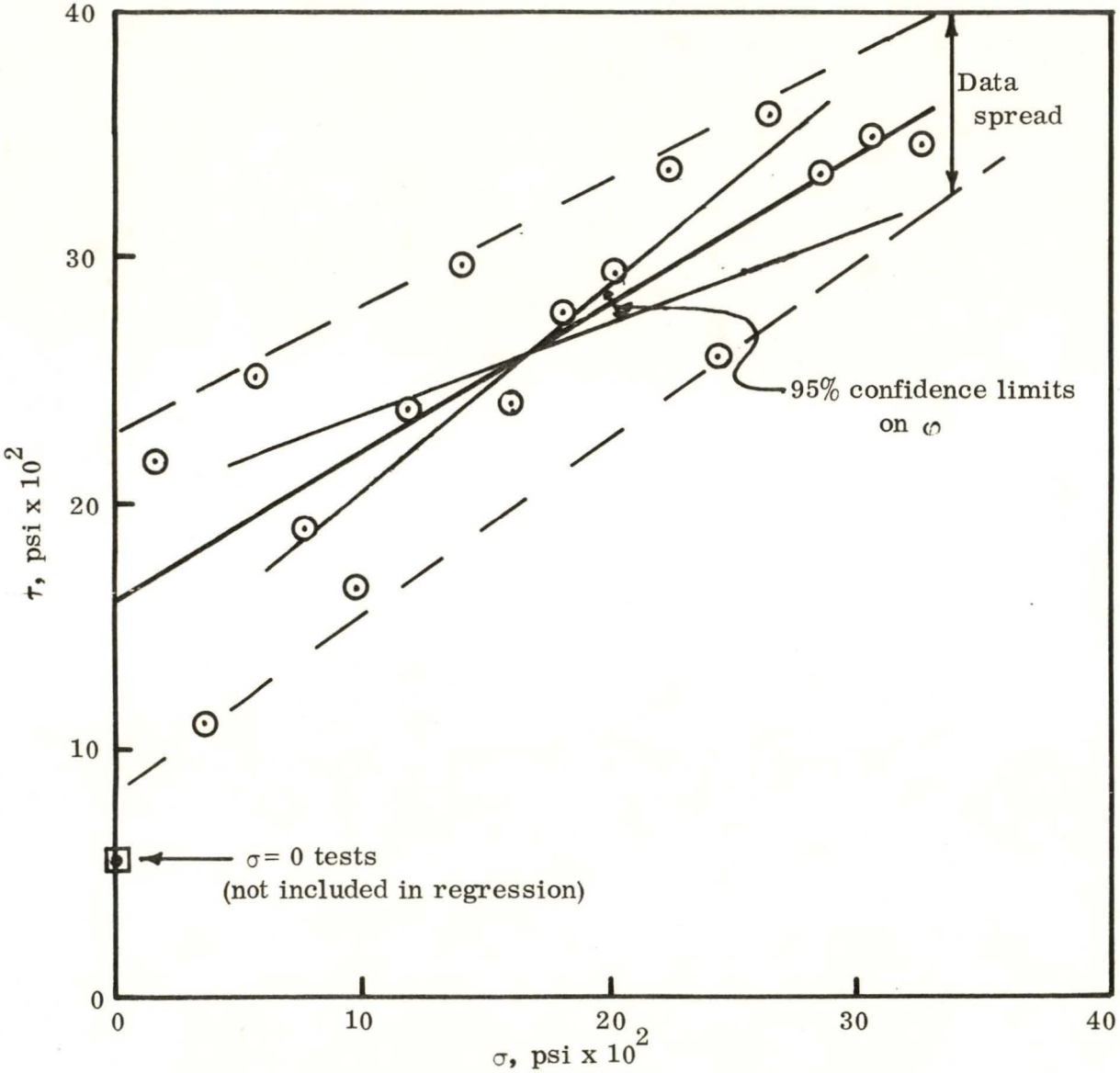

Figure 9. Double direct shear test results, shearing parallel to bedding.

Direct Shear with Zero Normal Stress. For comparison eleven cores taken in each direction were sheared in the same double direct shear device but with $\sigma = 0$. Results were as follows:

Parallel to bedding planes, $\sigma = 0$, $\tau = 535 \pm 124$ psi.

Normal to bedding planes, $\sigma = 0$, $\tau = 1520 \pm 326$ psi.

The $\pm$ values indicate 95% confidence limits on the means. A significant difference is apparent, the shear strength across the bedding planes being much higher, but still less than the cohesions obtained by regression analyses of the direct shear data with σ unequal to zero. Thus it appears that cohesion cannot be reliably measured by double shear test with $\sigma = 0$. Of even greater significance, the cohesion developed under low normal stress is not dependable because of the liklihood of shearing along fractures or bedding planes. This tendency also is shown by the increasing vertical spread of the data set in Figure 9 at low normal stresses.

Triaxial Shear. Triaxial shear tests were conducted on 2 1/8 in. diameter by 4 in. cores. The percentage recovery of usable cores varied from 71% for those cut parallel to the bedding planes to only 18% for those cut perpendicular, suggesting that the latter group in particular may be non-representative because of survival of the strongest. The minor principal stresses σ_3 ranged from about 500 to 1800 psi, Fig. 10. The Mohr circles contact the failure envelope in the σ range 1500 to 3500 psi, coinciding with the upper range of σ's of the bore-hole shear test.

For greater convenience of statistical analysis, the triaxial shear data were analyzed by regressing the maximum shearing stress, $q = \frac{1}{2}(\sigma_1 - \sigma_3)$ against the mean principal stress, $p = \frac{1}{2}(\sigma_1 + \sigma_3)$. The slope $\tan \alpha$ and intercept $\underline{a}$ of the resulting regression equation relate to ϕ and c as follows:

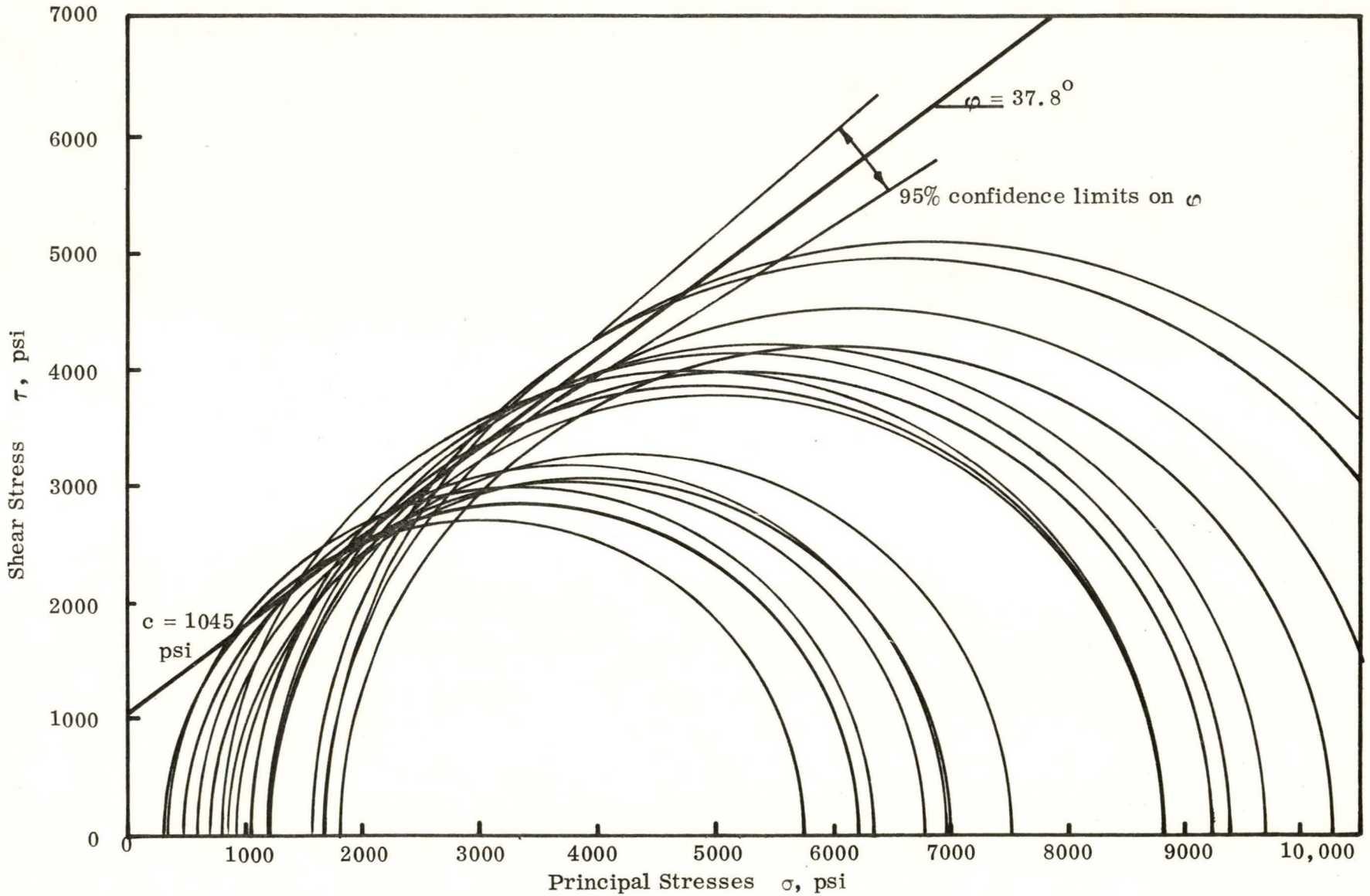

Figure 10. Mohr circles from triaxial shear tests of coal.

$$\sin \varphi = \tan \alpha \tag{11}$$

and

$$c = \frac{a}{\cos \varphi} \tag{12}$$

Results are presented in Table IV. The friction angle is higher than obtained from the other tests, 37.8^{o}, and the 95% confidence band range from 18 tests is 6.6^{o}, about one-third of the range from 16 direct shear tests and also less than from either set of 16 conventional bore-hole shear tests. Confidence bands overlap on φ from all three types of tests. It should be noted that the direction of shearing in the triaxial test is nominally inclined $45^{o} + \varphi/2$ to the minor principal stress axis, and thus is neither parallel nor perpendicular to the bedding planes. This should tend to reduce variability and increase strength. Perhaps significantly, the variability of the bore-hole shear conventional test data for $\bar{\varphi}$ was much higher with shearing parallel to the bedding than perpendicular to the bedding, and in fact the variability of the latter is closely comparable to that obtained from the triaxial tests. This suggests that variability of the various tests does not reflect test imprecision so much as the variable and anisotropic coal samples. A confirmation of this can be seen in the close agreement of tests on plaster, Appendix E. In comparing the coal test results one must also keep in mind the probable biasing of the triaxial test results upwards because of disintegration of the weaker cores.

Summary: Comparative Shear Test Data on Coal

The results from bore-hole shear, direct shear, and triaxial tests on the Lovilia coal are summarized in Table V. The mean friction angle obtained from bore-hole shear tests is between the means from direct shear and triaxial tests, and may be

Table IV

Triaxial Shear Data for Lovilia Coal

σ_1 parallel to bedding		σ_1 perpendicular to bedding	
$p = \frac{1}{2}(\sigma_1 + \sigma_3)$ psi	$q = \frac{1}{2}(\sigma_1 - \sigma_3)$ psi	$p = \frac{1}{2}(\sigma_1 + \sigma_3)$ psi	$q = \frac{1}{2}(\sigma_1 - \sigma_3)$ psi
Series 1			
3355	2995	6812	5122
5193	4153	3313	2803
6534	4964	3904	3074
3015	2716	5438	4248
3787	3187		
4801	3991		
5005	3785		
6012	4202		
Series 2			
6208	4518		
3355	2865		
5197	3997		
4915	3885		
3729	3029		
4223	3293		

Summary: Parallel to bedding,

$\tan \alpha = 0.5890$

$a = 932$

$\varphi = 36.1^{\circ}$

$c = 1154$ psi

Perpendicular to bedding,

$\tan \alpha = 0.6645$

$a = 598$

$\varphi = 41.6^{\circ}$

$c = 800$ psi

All data:

$\tan \alpha = 0.6132$

95% C.I. $= \pm 0.04496$

$a = 825.7$

$\varphi = 37.8^{\circ}$

95% C.I. $= 34.6 - 41.2^{\circ}$

$c = 1045$ psi

Table V

Comparative Test Results

	Bore-Hole[b]	Double Direct	Triaxial
Shearing Parallel to Bedding[a]			
$\bar{\varphi}$	32.6°	31.6°	----
95% C.I. on $\bar{\varphi}$	25-40°	21-40°	----
Range	18.2°	21.9°	----
$\bar{c}$	22.3 psi	1611 psi	----
Shearing Perpendicular to Bedding			
$\bar{\varphi}$	31.5°	29.1°	----
95% C.I. on $\bar{\varphi}$	27-36°	18-38°	----
Range	9.8°	23.3°	----
$\bar{c}$	47.9 psi	2151 psi	----
Shearing Inclined to Bedding			
$\bar{\varphi}$	----	----	37.8°
95% C.I. on $\bar{\varphi}$	----	----	35-41°
Range	----	----	6.6°
$\bar{c}$	----	----	1045 psi
All Respective Tests			
$\bar{\varphi}$	32.0°	30.4°	37.8°
95% C.I. on $\bar{\varphi}$	27-37°	23-37°	35-41°
Range	10.4°	14.5°	6.6°
$\bar{c}$	35 psi	1881 psi	1045 psi

[a] $\bar{\varphi}$ = mean friction angle φ; $\bar{c}$ = mean cohesion c.

[b] Conventional tests only.

determined in situ in much less time. Precision of the bore-hole test for determining ϕ with shearing across the bedding is comparable to precision of the triaxial test, and appears to be strongly influenced by sample variability. The cohesion from bore-hole shear tests in only a fraction of that from the other tests, and probably represents pulverized and repacked coal.

Attempts to Improve Measurement of Cohesion

Several series of bore-hole shear tests were conducted using special procedures to improve the seating of shear plate corrugations into the coal, still without actually pre-grooving with a special cutter. The tests previously described have been designated Series A Tests; the special series are as follows:

Series B Tests: normally stressed-vibrated
The expansion head was inserted into the sample; a normal pressure was set and any shear stresses which developed during normal pressure application were relieved. The gear of the pulling unit was turned back such that the pulling rod and expansion head were supported only by the shear plates engaging material. Then the top of the pulling rod was briskly struck five times with a rubber mallet in an attempt to vibrate the shear plates into the coal. The shear stress was then increased to a maximum.

Series C Tests: overstressed-nonvibrated
In general, the expansion head was inserted into the sample and a normal stress was applied higher than that normal stress at which the sample was to be sheared. The normal stress was then decreased to a value less than that designated for shear to relieve any residual normal stress from the overstressing portion of the test. The normal stress for shear was set and the area was failed.

Series C1 Tests: overstressed to σ = 2918 psi.

Series C2 Tests: overstressed to σ = 3413 psi.

Series C3 Tests: overstressed to σ = 39 08 psi

Series D Tests: overstressed-vibrated

These tests were combinations of Series B and Series C tests. The pulling rod was struck five times with the rubber mallet while the overstressing pressure was acting. Series D1, D2, and D3 tests had the same overstressing pressures as did Series C1, C2, and C3, respectively.

The method for interpretation of these tests (Fig. 11) was to establish φ from conventional test data subsequent to the first point, which was found to be the only point affected by pre-shear seating attempts. A line with this φ angle was then fitted through the first data point, and the calculated intercept on the τ axis is designated c_i, cohesion from the initial data point. Results are presented in Appendix G and are summarized in Table VI.

As can be seen in Table VI, the several pre-shear techniques all tended to increase average values measured for cohesion by ratios of 1.25 to 3 times, but the values are still low compared to the 1000-2000 psi realized from laboratory tests. The highest value for c_i from all 40 series B, C, and D tests is 623 psi for a series B test sheared perpendicular to the bedding planes (Sample S, Appendix F). This is about two-thirds of the value obtained from triaxial tests, and suggests that further improvement should be possible, perhaps by vibrating while under a high applied normal stress.

Perhaps equally significant, the various pre-shear treatments also increased measured friction angles about 3 degrees. The mean φ from all 40 special pre-shear technique tests is $35.2^0 \pm 5.2^o$, compared to 32 ± 5.2^o from the previous bore-hole shear tests and 38 ± 3.3^o from triaxial tests. Further research and instrument modification, perhaps incorporating a remotely actuated hammer or vibrator in the shear head, appears desirable.

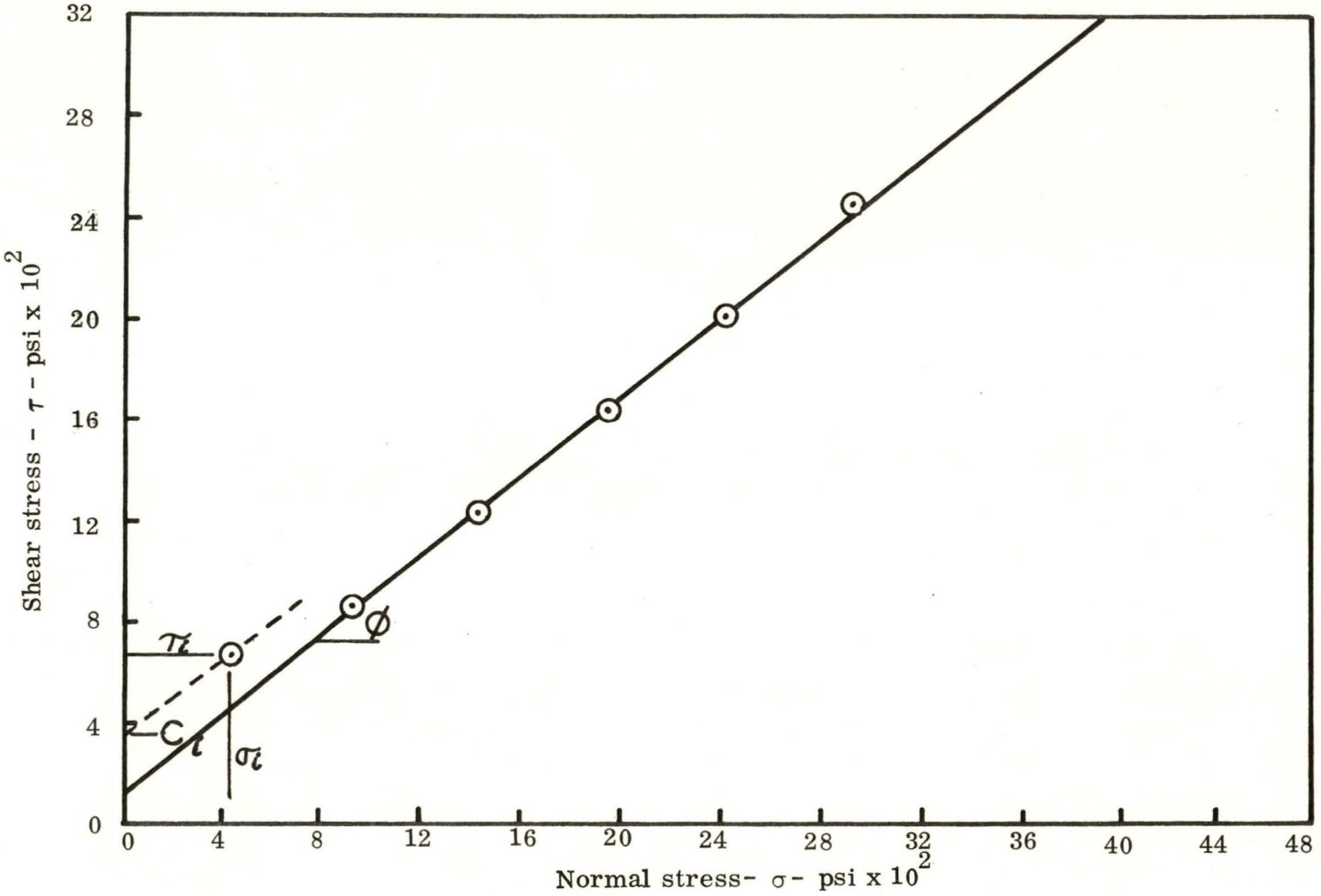

Figure 11. Effect of preshear technique on determination of cohesion. Series D1, Sample E2.

Table VI. Summary of Influence of Pre-Shear Technique on Bore-Hole Shear Cohesion

Series	Pre-Shear Technique	No. of Tests		ϕ, ^{o}	c_i, psi
A	None	15		32.7	88[a]
B	Hammer blows	15		34.3	110
C1	Overstressed to 2918 psi	4		34.5	211
C2	Overstressed to 3413 psi	5		34.5	211
C3	Overstressed to 3908 psi	4		36.6	232
			Av.	35.2	218
D1	Hammer blows at 2918 psi	4		38.1	235
D2	Hammer blows at 3413 psi	4		35.8	314
D3	Hammer blows at 3908 psi	4		35.4	254
			Av.	36.4	268

[a] Mean from conventional tests.

CONCLUSIONS

1. An apparatus was designed and built to perform shear testing of coal from inside a 3-inch diameter hole left by coring. The normal pressure and the shearing stress can be independently varied to give a measure of the cohesion and friction parameters of the coal. Contact with the coal is by two 1-inch x 2-inch long curved and sharply corrugated shear plates. The normal stress range is up to 5000 psi, the shearing stress up to 10,000 psi.

2. Apparatus friction may be accounted for by shearing stress and normal stress calibrations, which resulted in superposition of the friction angles obtained during increasing-normal-stress and pull vs. decreasing-normal-stress and rebound tests, using the appropriate calibration curves.

3. Cohesions measured by bore-hole shear tests without pre-stressing are very low and appear to reflect cohesion of the pulverized and repacked coal.

4. Friction angles measured by the bore-hole shear tester for Lovilia, Iowa, coal are closely comparable to those obtained by direct shear or by triaxial testing: that is, for all tests regardless of orientation, the approximate $\bar{\varphi}$ angles and 95 percent confidence intervals from comparable numbers of tests are:

Bore-hole shear	$\bar{\varphi}$	$= 32 \pm 5^{o}$
Direct shear	$\bar{\varphi}$	$= 30 \pm 7^{o}$
Triaxial shear	$\bar{\varphi}$	$= 38 \pm 3^{o}$

The range in values represented by the $\pm$ notation includes variability of the coal, which in turn depends on shear plane orientation with respect to bedding planes.

5. Preliminary overstressing and hammering of the shear device to promote seating of the shear plate teeth increased measured cohesions several fold and measured friction angles to

$$\text{Prestressed bore-hole shear } \bar{\phi} = 35 \pm 5^{o},$$

significantly closer to the triaxial test average.

FUTURE RESEARCH

The application of the bore-hole shear principle to the testing of coal appears quite promising, and several avenues are open for research to further perfect the test:

1. Modify the device to reduce friction and simplify construction. This is desirable from the standpoint of cost, and the need for re-calibration should the friction change. Possibilities include revising or eliminating the pressure intensifier for the shear head, introduction of a stress transducer between the shear plates and the hydraulic system, and changing from a regulated CO_2 to a hand-operated hydraulic expansion system to save weight.

2. Modify the device to improve plate seating. This appears desirable both from the standpoints of measured cohesion and angle of friction. It should be noted that a valid measure of cohesion requires only that the first shearing induce fracture of coal between the points of the contact teeth, and should not require full embedment of the points. A high frequency low amplitude "hard" (square, saw-tooth or impact wave) vibration might effectively secure the necessary embedment with a minimum of fracturing.

3. Extend the tests to other coals. This is essential to prove general worth of the method; perhaps the data agreements noted are an auspicious coincidence holding only for Lovilia, Iowa coal.

DISCUSSION: STRENGTH PARAMETERS PERTINENT TO DESIGN

The friction angle obtained from the bore-hole shear device probably describes sliding of pulverized and compacted coal over a sheared coal surface, and thus is mainly sliding friction without much dilatancy or "interlocking" component. The bore-hole shear friction angle therefore should be somewhat lower than that obtained from triaxial tests at relatively low stress levels, but on the safe side for design.

Cohesion of coal is strongly influenced by the direction of shearing relative to directions of microfracturs and bedding planes, and by specimen size because of the increased probability of encountering adversely oriented microfractures in larger specimens, which raises a question as to how much cohesion should be relied upon for design of coal pillars, or whether it should be relied upon at all.

REFERENCES

1. Barry, Anthony J. and Oscar B. Nair. In-situ tests of bearing capacity of roof and floor in selected bituminous coal mines: A progress report-longwall mining. U. S. Bureau of Mines, Report of Investigations 7406, 1970.

2. Bowden, F. P. and K. Tabor. The friction and lubrication of solids, Part I. Oxford, Clarendon Press. 1950.

3. Brown, J. H. and C. D. Pomeroy. Friction between coal and metal surfaces. In W. H. Walton, ed. Mechanicsl properties of non-metallic brittle materials. Pp. 419-431. New York, New York, Interscience Publishers, Inc. 1958.

4. Caudle, Rodney Duane and G. B. Clark. Stresses around mine openings in some simple geologic structures. University of Illinois Engineering Experiment Station. Bull. 430. 1955.

5. Coulomb, C. A. Essai sur une application des regles de maximis and minimis a quelques problemes de statique relatifs a l'architecture, Academie Royale des Sciences, Paris, France. Memoires 7: 343-382. 1776.

6. Dumbleton, M. J., M. J. O'Dogherty and R. Shepard. The effects of blade angle and other factors on coal ploughing. In W. H. Walton, ed. Mechanical properties of non-metallic brittle materials. Pp. 432-450. New York, New York, Interscience Publishers, Inc. 1958.

7. Easton, Charles Newton. An in-place shear strength testing method for subaqueous soils. Unpublished M.S. thesis. Ames, Iowa, Library, Iowa State University of Science and Technology. 1968.

8. Evans, I. Theoretical aspects of coal ploughing. In W. H. Walton, ed. Mechanical properties of non-metallic brittle materials. Pp. 451-468. New York, New York, Interscience Publishers, Inc. 1958.

9. Evans, I. and S. A. F. Murrell. The forces required to penetrate a brittle material with a wedge-shaped tool. In W. H. Walton, ed. Mechanical properties of non-metallic brittle materials. Pp. 432-450. New York, New Yor, Interscience Publishers, Inc. 1958.

10. Evans, I. and C. D. Pomeroy. The strength of cubes of coal in uniaxial compression. In W. H. Walton, ed. Mechanical properties of non-metallic brittle materials. Pp. 5-28. New York, New York, Interscience Publishers, Inc. 1958.

11. Fox, Nathaniel Sill. Soil shear test device for use in bore holes. Unpublished M.S. thesis. Ames, Iowa, Library, Iowa State University of Science and Technology. 1966.

12. Jaeger, J. C. The brittle fracture of rocks. In Charles Fairhurst, ed. Failure and breakage of rock-eight symposium on rock mechanics. Pp. 3-58. Baltimore, Maryland, Port City Press, Inc. 1967.

13. Jaeger, J. C. Elasticity, fracture, and flow with engineering and geological applications. Second edition. New York, New York, John Wiley and Sons, Inc. 1956.

14. Johnston, C. M. and E. S. Barber. A compendium on testing apparatus. In Roy W. Crum, ed. Soil mechanics and soil stabilization, Part II. Pp. 371-426. Proc. 18th Annual Meeting, Highway Res. Board. Washington, D.C., Highway Res. Board. 1938.

15. Lajtai, E. Z. Strength of discontinuous rocks in direct shear. Geotechnique 19, No. 2:218-233. June. 1969.

16. Lambe, T. William. Soil testing for engineers. New York, New York, John Wiley and Sons, Inc. 1969.

17. Lambe, T. William and Robert V. Whitman. Soil mechanics. New York, New York, John Wiley and Sons, Inc. 1969.

18. Obert, Leonard. An inexpensive triaxial apparatus for testing mine rock. U.S. Bureau of Mines, Report of Investigations. 6332. 1963.

19. Obert, Leonard and Wilbur I. Duvall. Rock mechanics and the design of structures in rock. New York, New York, John Wiley and Sons, Inc. 1967.

20. Obert, Leonard, R. L. Merrill and T. A. Morgan. Bore-hole deformation gauge for determining the stress in mine rock. U. S. Bureau of Mines, Report of Investigations. 5978. 1962.

21. Panek, L. A. and J. A. Stock. Determination of the modulus of rigidity of rock by expanding a cylindrical pressure cell in a drill hole. Proc. 6th Symp. Rock Mech., Rolla, Missouri. Pp. 427-449. University of Missouri, Rolla. 1964.

22. Panek, L. A. and J. A. Stock. Development of a rock stress monitoring station based on the flat slot method of measuring existing rock stresses. U. S. Bureau of Mines, Report of Investigations. 6537. 1964.

23. Paulding, B. W. Jr. Techniques used in studying the fracture mechanics of rock. In Testing techniques for rock mechanics. ASTM Spec. Tech. Pub. No. 402. Philadelphia, Pennsylvania, American Society for Testing and Materials. 1966.

24. Protod'yakonov, M. M., M. I. Koifman and others. Mechanical properties of rocks. Jerusalem, Israel Program for Scientific Translations, Ltd. 1969.

25. Seeley, Fred B. and James O. Smith. Advanced mechanics of materials. Second edition. New York, New York, John Wiley and Sons, Inc. 1932.

26. Skempton, A. W. Terzaghi's discovery of effective stress. In L. Bjerrum and others, eds. From theory to practice in soil mechanics. Pp. 42-53. New York, New York, John Wiley and Sons, Inc. 1960.

27. Stagg, K. G. and O. C. Zienkiewicz. Rock mechanics in engineering practice. New York, New York, John Wiley and Sons, Inc. 1968.

28. Stagg, K. G. and O. C. Zienkiewicz. The cable method of in situ testing. Intern. J. Rock Mech. Mining Sci. 4:273-300. 1967.

29. Terzaghi, K. Theoretical soil mechanics. New York, New York, John Wiley and Sons, Inc. 1943.

30. Timoshenko, S. and J. N. Goodier. Theory of elasticity. New York, New York, McGraw-Hill Book Company, Inc. 1951.

ACKNOWLEDGEMENTS

This work was supported by the Engineering Research Institute, Iowa State University, through funds made available by the U. S. Department of Interior, Bureau of Mines, under grant number G1010745 (MIN-46). The authors express their thanks to the Iowa Department of Mines and Minerals and to Mr. Thomas Wignalls, owner and operator of the Lovilia Coal Company, for arranging for collection of coal samples used for this research.

APPENDIX A

Design and Operation of a High-Pressure Triaxial Apparatus

An inexpensive triaxial apparatus was constructed on the basis of similar devices reported in the literature (18). Figure A1 shows the triaxial cell, consisting of a thick-walled cylinder and two end loading platens which also act as seals. A cylindrical core 2 1/8 inches in diameter and 4 inches long is enclosed in two thick-walled rubber membranes and secured to only the lower platen. A 1/4-inch-thick steel disc having the same diameter as the sample is fixed to the top of the sample. The axial load is transmitted to the sample through a flat washer which rests on the steel disc. This procedure allows the lateral pressure to act on the top of the sample.

The cell is assembled and placed in a compression testing machine. Before lateral pressure is applied, the loading head is brought down on the upper platen until 50 pounds load is noted. A dial gauge to show axial deformation is then set to zero. A 10:1 ratio pressure intensifier using CO_2 gas on the low-pressure side and hydraulic oil on the high-pressure side supplies the confining pressure. As the confining pressure is applied, the dial gauge decreases to a negative value as the upper platen lifts off the sample; the upper platen is brought back down on the sample by loading until the dial gauge has returned to zero.

Load, deformation and confining pressure are monitored during the test. Because the pressure regulator is on the low-pressure side of the intensifier, confining pressures were found to vary about 10 percent from the initial setting during the test. The values at failure are used in the analysis.

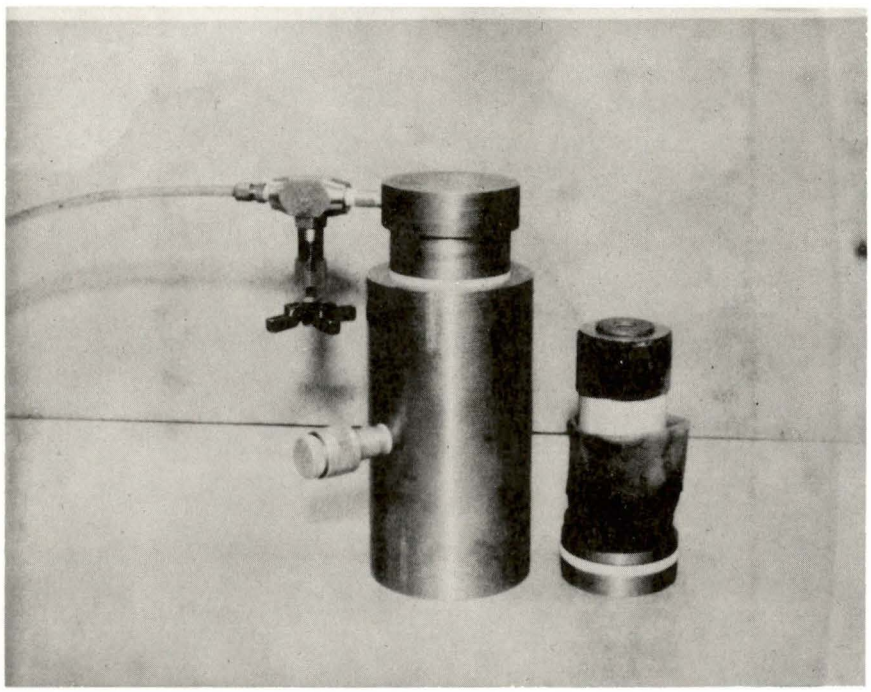

Figure A1. High pressure triaxial cell.

Sample Preparation

Samples for triaxial shear tests were cored with a diamond core barrel and then cut to approximate length with a diamond rock saw. To insure parallel and uniform ends the samples were then dressed down in a surface grinder as shown in Figure A2. Use of the surface grinder for final preparation allowed sample length to be maintained within 0.01 inch.

Detailed Apparatus Description

Some characteristics of the triaxial tests used in this research are as follows:

1. The cell is capable of confining pressures up to 10,000 psi.

2. Elevated confining pressures require special seals to restrain the confining fluid. High pressure seals result in frictional forces which must be taken into account.

3. All samples are tested dry because excess pore pressures can neither be measured nor eliminated in that the sample is sealed within the cell.

4. The major principal stress, σ_1, is measured directly.

5. No weights can be applied to the top platen to prevent its being lifted during confining pressure application.

6. The cross-sectional area of the triaxial cell must be known, for reasons discussed below.

To determine the cell cross-sectional area and evaluate the magnitude of the frictional forces caused by high pressure seals, a cell calibration is performed. Having been filled with fluid and placed in the loading machine, the cell is pressurized at various pressure intervals and the load registered by the machine for each pressure is noted.

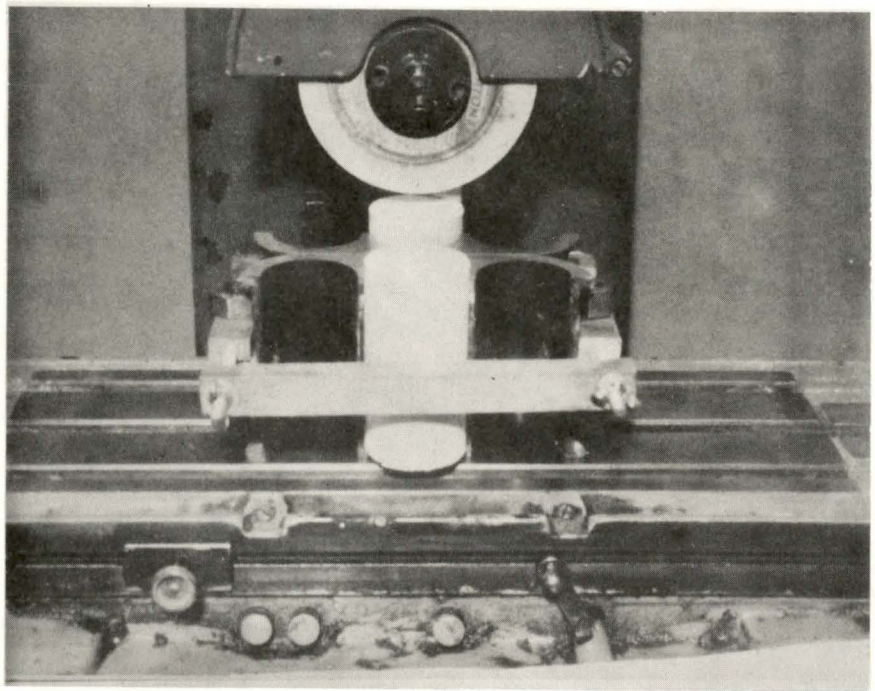

A2. Device to prepare triaxial samples.

Since force equals pressure times area, if the load in pounds is plotted versus the pressure in the cell, the slope of the resulting straight line is the cell cross-sectional area determined more accurately than by direct measurement. The intercept, which is positive, represents the frictional resistance in pounds due to the action of the high pressure seals on the inside walls of the cell.

During an actual triaxial test, the loading machine measures both the sample and the circumferential fluid forces acting on the ends of the cell. Thus the confining pressures acting vertically on the cell are automatically converted to pounds load by the loading machine. Therefore, neither the frictional force nor the force acting over the area defined by the area of the cell minus the area of the sample contribute to the major principal stress on the sample.

In addition, because the sample is sealed within the chamber, a constant sample volume is assumed. Thus the cross sectional area of the sample is assumed to change during the test according to the relationship

$$A = \frac{A_o}{1 - \epsilon} \tag{1}$$

where: A_o = the original sample cross sectional area

ϵ = the axial strain, and

A = the new cross sectional area.

The major principal load can be expressed as

$$P = P_t - P_f - P_{ad}, \tag{2a}$$

where: P = the actual vertical load acting on the sample,

P_t = the load indicated by the loading machine,

P_f = the load due to seal friction as determined by the calibration procedure, and

P_{ad} = the monitored load due to the chamber and the sample area difference.

Then

$$P_{ad} = \sigma_3 (A_c - A).$$

where: σ_3 = confining pressure,

A_c = cross sectional area of the chamber.

Substituting from (1) and (2a),

$$P_{ad} = \sigma_3 (A_c - \frac{A_o}{1 - \epsilon})$$

$$P = P_t - P_f - \sigma_3 (A_c - \frac{A_o}{1 - \epsilon}) \tag{2b}$$

The major principal stress σ_1 acting on the sample is

$$\sigma_1 = \frac{P_t - P_f - \sigma_3 (A_c - \frac{A_o}{1 - \epsilon})}{A_o / (1 - \epsilon)} \tag{3}$$

Equation 3 was used to evaluate the major principal stress for all triaxial work. A cell calibration was conducted each day triaxial tests were performed in case the seal friction might change with either apparatus use or disuse.

APPENDIX B

High-Pressure Direct-Shear Apparatus

The high-pressure direct-shear apparatus for 1-inch diameter rock cores is similar in design and operation to the Arizona double shear device by O'Harra (14). The double direct shear device consists of a sliding plate arrangement (Fig. B1) through which a cylindrical sample is inserted. The normal stress, σ, is applied at one end of the sample with a Bellofram-sealed piston, and has a maximum normal stress capacity of 3,300 psi. The shearing stress is applied with a compression loading machine such that the cross sectional area is sheared twice; hence the term double direct shear. As in the triaxial test, the direction of shear with respect to the bedding planes is governed by the direction the core is taken; and similar to other direct shear devices, the failure plane is fixed at the junctions between the center plate and the adjacent plates.

Two basic design considerations were important for the direct shear apparatus:

1. Flexural stresses should be minimized or eliminated.

2. Radial stress concentrations resulting from the discontinuity between the sample and the apparatus should be minimized.

Flexural stresses are minimized by the shear plate design and by elastic bending of the core, as shown in Fig. B2(a) and B2(b), where the couple Fx reduces as stresses become non-uniform. Radial stress concentrations are shown in Fig. B3. Dividing the shear load in pounds by twice the cross sectional area of the sample (double shear) assumes the shear stress distribution is uniform along the diameter as shown in Fig. B3(b).

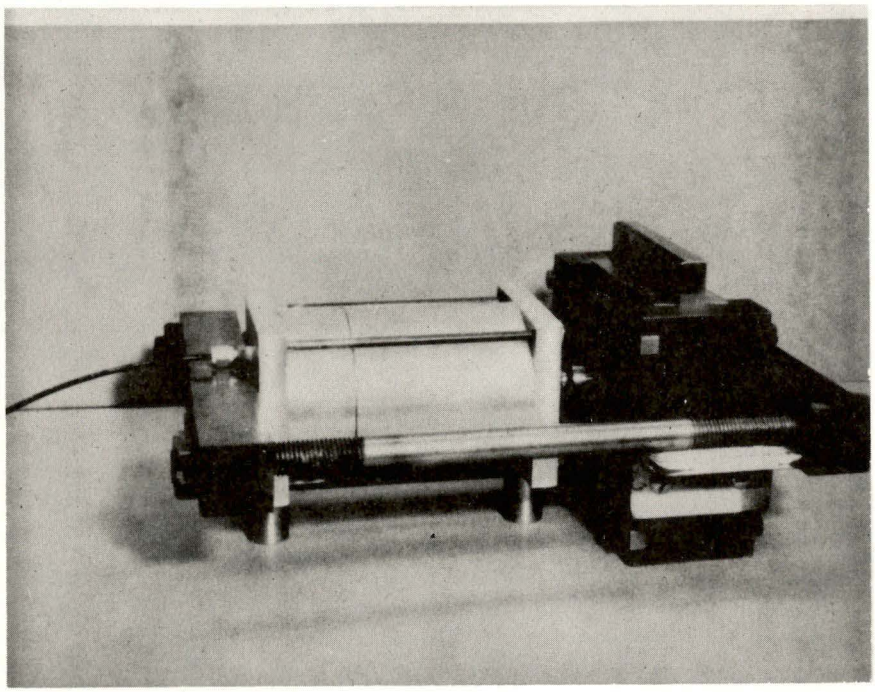

Figure B1. High pressure direct-shear device.

This procedure would be acceptable provided the sample were an integral part of all three shear plates. However, the sample diameter is less than the diameter of the hole in the plates and the shearing stress at the center is the greater than at the ends of the horizontal diameter. Because the device was used primarily to compare angles of internal friction and not cohesions, the stress concentration factor was not determined. Within the realm of a linear failure envelope, the angle of internal friction should be independent of stress concentration. On the other hand, the measured cohesion will be reduced because of progressive failure.

a

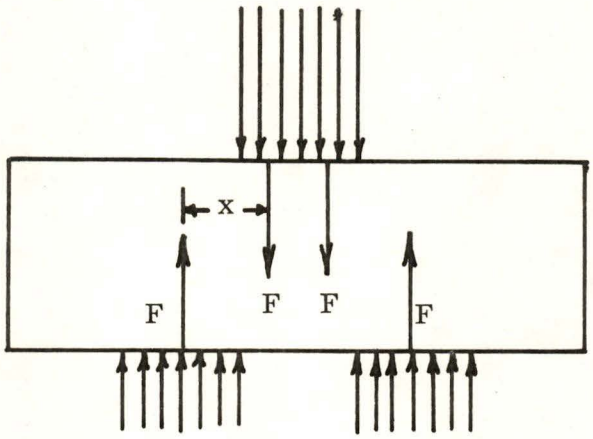

b

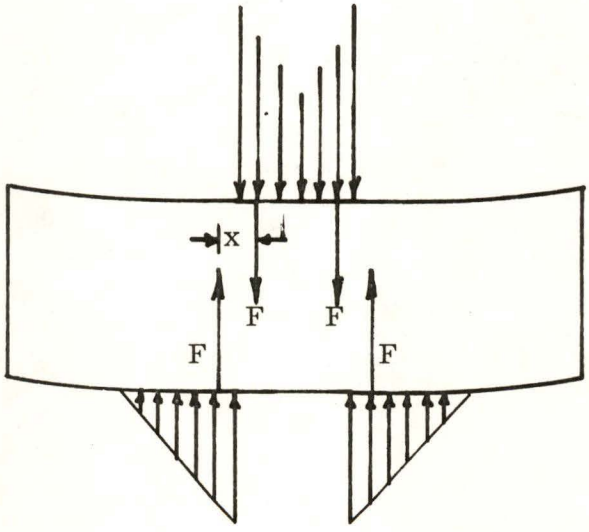

Figure B2. Longitudinal stress distributions in double direct shear samples.

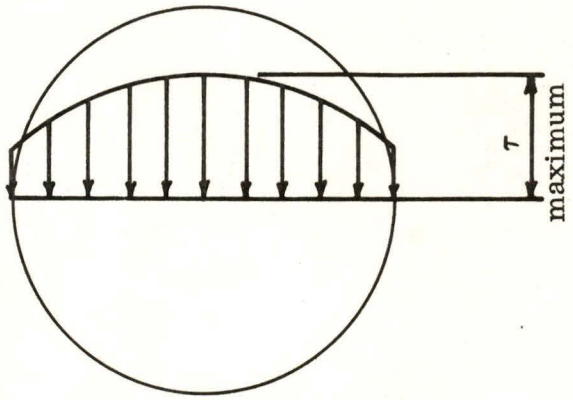

B3(a). Probable shear stress distribution

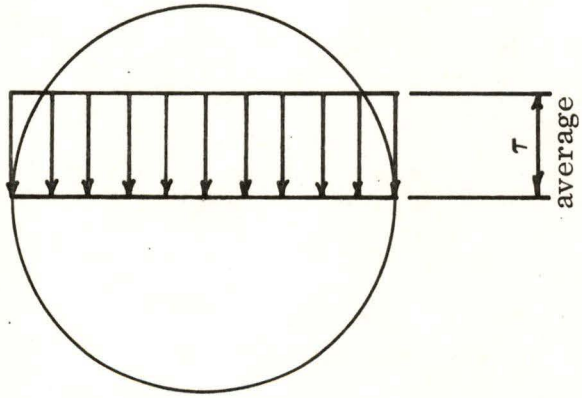

B3(b). Assumed shear stress distribution

Figure B3. Transverse stress distributions in double direct shear samples.

APPENDIX C

Derivation of a Criterion for Slippage vs. Shear

The corrugation interlocking system shown in Figure C1 gives idealized horizontal and vertical forces acting on an individual asperity indicated in Figure C2. These forces multiplied by the number of asperities give F and $\dot{N}$, respectively.

The forces applied to side a-b of the asperity in Figure C2 can be separated into components parallel and perpendicular to the surface.

$$pa_1 = n \sin \theta$$

$$pa_2 = f \cos \theta$$

$$pe_1 = n \cos \theta$$

$$pe_2 = f \sin \theta$$

Summing forces parallel to side a-b gives

$$PA = f \cos \theta - n \sin \theta$$

Summing forces perpendicular to side a-b gives

$$PE = f \sin \theta + n \cos \theta$$

By rotating side a-b, θ degrees counterclockwise, the sliding block analogy shown in Figure C3 can be applied. If slippage is impending, the following equation will describe the forces on surface a-b:

$$f' = n'\mu$$

where μ is equal to the coefficient of static friction between the block and the surface. The numerical value of μ is equal to tan φ_μ, where φ_μ is the angle of friction. By substitution

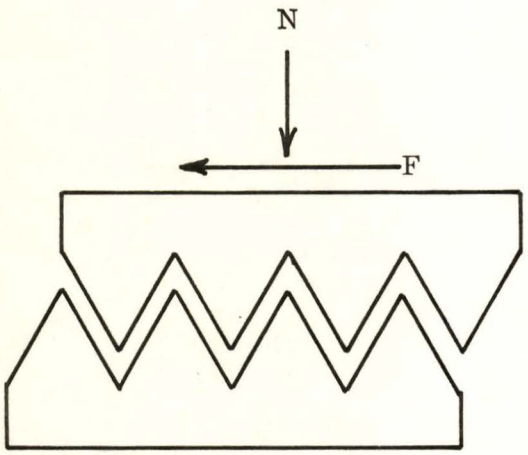

Figure C1. Corrugation interlocking system.

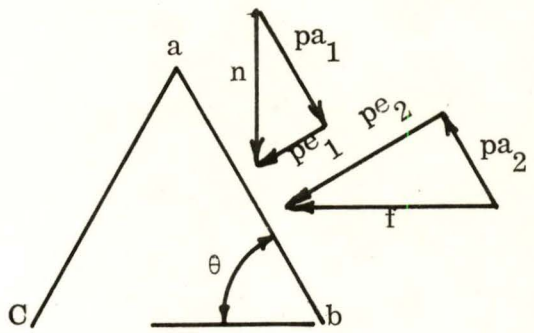

Figure C2. Forces on an individual asperity

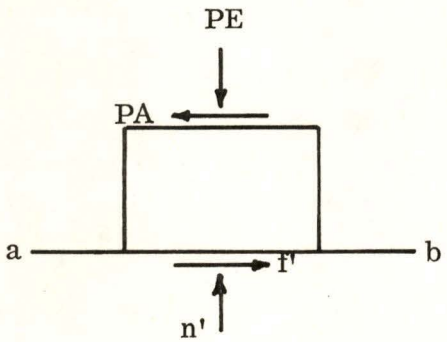

Figure C3. Sliding block analogy.

$$\tan \varphi_\mu = \frac{f'}{n'} = \frac{PA}{PE} = \frac{f \cos \theta - n \sin \theta}{n \cos \theta + f \sin \theta}$$

Dividing both the numerator and denominator of this expression by cos θ gives

$$\tan \varphi_\mu = \frac{f - n \tan \theta}{n + f \tan \theta}$$

Cross multiplying allows a solution for f which is

$$f = \frac{n (\tan \varphi_\mu + \tan \theta)}{1 - \tan \theta \tan \varphi_\mu}$$

Employing the appropriate trigonometric identity gives

$$f = n \tan (\theta + \varphi_\mu)$$

Since the magnitudes of the externally applied forces, F and N, were divided by the number of asperities to give f and n, respectively, multiplication by that same number will give

$$F = N \tan (\theta + \varphi_\mu) \qquad \text{(C1)}$$

Equation C1 is an expression for the force required to cause slipping.

The Mohr-Coulomb failure criterion, $\tau = c + \sigma \tan \varphi$, is an expression for the stresses on the shear failure plane represented by bc in Fig. C2. If we assume F and N are evenly distributed across the shear area, A_s,

$$\frac{F}{A_s} = \frac{N}{A_s} (\tan \theta + \varphi_\mu)$$

or

$$\tau = \sigma \tan (\theta + \varphi_\mu)$$

Together with the Mohr-Coulomb failure criterion, the above equation gives the criterion for material failure before slippage of the shear plate:

$$\tau = c + \sigma \tan\varphi < \sigma \tan(\theta + \varphi_\mu) \tag{C2}$$

Dividing Equation C2 by σ and rearranging results in

$$c/\sigma < \tan(\theta + \varphi_\mu) - \tan\varphi \tag{C2a}$$

APPENDIX D

Correction of c and φ for Opening Friction During Pulling

1. Friction present when the head is not being pulled is accounted for by using appropriate calibration curves for opening or closing.

2. Friction during pulling subtracts from σ during opening of the shear head, or adds to σ during closing. Assuming friction is equal in both directions, the effect on σ is as shown in Fig. D1, from which

$$\cot \varphi = \frac{b}{d} \rightleftharpoons \frac{a + c}{2d}$$

$$= \frac{1}{2} \left(\frac{a}{d} + \frac{c}{d} \right)$$

$$= \frac{1}{2} (\cot \varphi_c + \cot \varphi_o) \qquad (1)$$

Cohesion may be evaluated by assuming the τ axis in Fig. D1 is moved to the right by an amount e; and downward an amount g; Fig. D2.

Then

$$\tan \varphi = \frac{g + c}{e}; \quad \tan \varphi_o = \frac{g + c_o}{e}; \quad \tan \varphi_c = \frac{g + c_c}{e};$$

from which

$$e = \frac{g + c}{\tan \varphi} = \frac{g + c_o}{\tan \varphi_o} = \frac{g + c_c}{\tan \varphi_c} \qquad (2)$$

Cross-multiplying the second two terms and solving for g,

$$g \tan \varphi_c + c_o \tan \varphi_c = g \tan \varphi_o + c_c \tan \varphi_o$$

$$g = \frac{c_c \tan \varphi_o - c_o \tan \varphi_c}{\tan \varphi_c - \tan \varphi_o} \qquad (3)$$

This value is then substituted into (2) to find c:

$$c = (c_o + g) \frac{\tan \varphi}{\tan \varphi_o} - g \qquad (4a)$$

or

$$c = (c_c + g) \frac{\tan \varphi}{\tan \varphi_c} - g \qquad (4b)$$

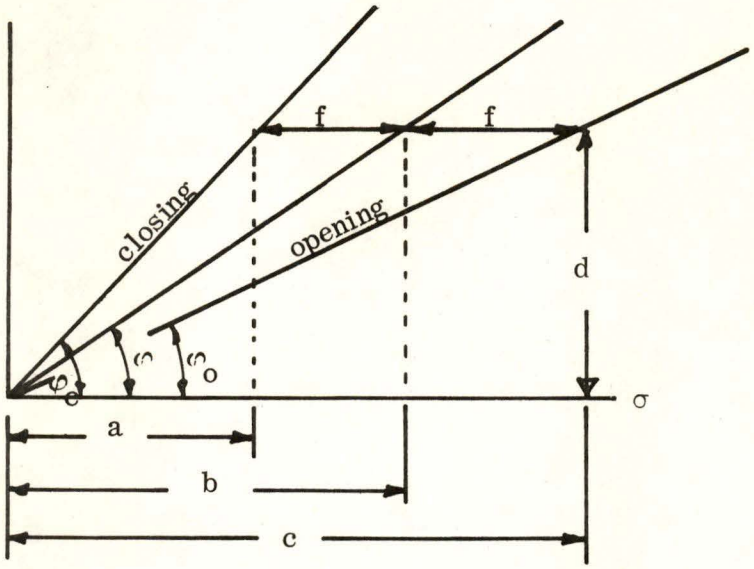

Figure D1.

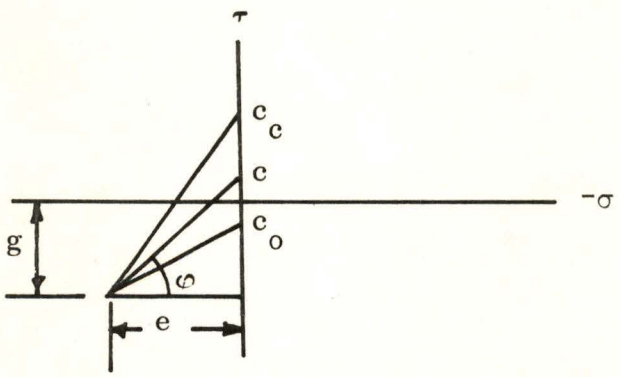

Figure D2.

APPENDIX E

Tests on Molding Plaster

Initial trials of the bore-hole shear and direct shear apparatuses were made on molding plaster. For the bore-hole shear tests, specimens were cast in six-inch diameter by seven-inch high steel molds used for the California Bearing Ratio test of soils (ASTM D1883-67). A three-inch outside diameter thin-walled steel (Shelby) tube was used to form the bore hole and was extracted before the material had completely set.

The model bore hole of some samples was grooved with the device shown in Figure E1. Attached to an electric drill, the device was rotated inside the bore hole to cut grooves corresponding to the corrugations on the shear plates. In some instances, complete grooves were not cut, but the bore hole surface was considerably roughened. Because the expansion head could not be precisely positioned in the sample, the degree of mating between the shear plate corrugations and the grooves could not be determined.

Direct Shear and Unconfined Compression

Typical double direct shear tests results on plaster are shown in Figure E2, along with Mohr circles obtained from unconfined compressive strengths of the same plaster. Triaxial tests were attempted but could not be interpreted because of drastic necking-down of the sample under pressure, amounting to about a one-third decrease in cross-sectional area and in volume. The direct shear results are very consistent and in close agreement with the unconfined compressive strengths, indicated by tangency

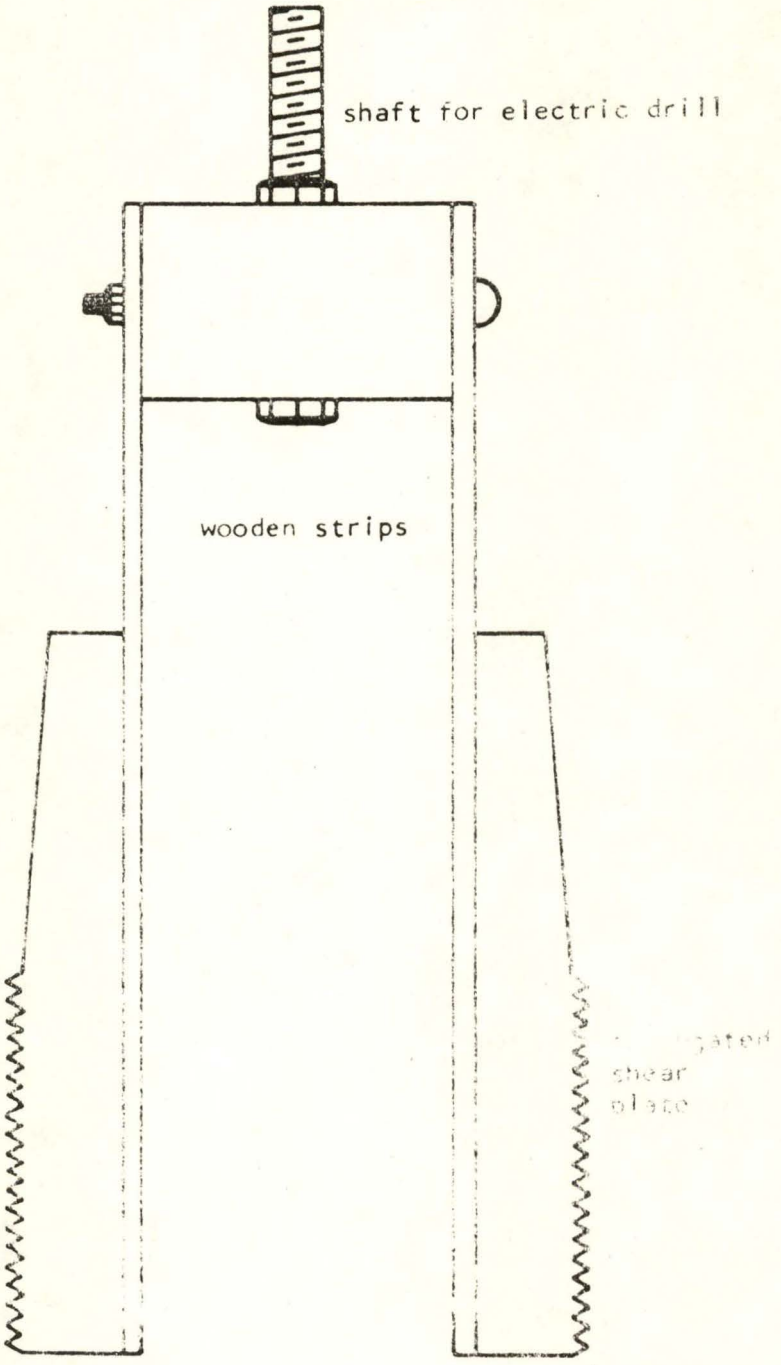

Figure E1. Grooving device used to prepare faces of model bore holes

around the top of the Mohr circle. The direct shear diagram is indicative of a cemented material, the low-σ part of the curve representing a primary cementation up to a breakdown of the cemented structure, resulting in lower strengths. At higher values of σ, strength is regained in proportion to σ, giving a valid friction angle φ. The structural breakdown hypothesized around the top of the Mohr circle is substantiated by the triaxial test experience. Plaster thus is not a good model for coal, being too porous and compressible.

The direct shear data are summarized in Table E1.

Bore-Hole Shear

Typical bore-hole shear data on plaster also are shown in Figure E2. This sample was pre-grooved and each point involved removing, cleaning, and relocating the shear head in an attempt to obtain a valid cohesion. Nevertheless the first point is below the direct shear test failure envelope, suggesting improper seating. However, point 2 in Figure E2 is on the envelope, and taken with Point 1 would give an incorrect φ, in this case 33^{o}. Points 3-7 are at stresses above that causing structural breakdown and give approximately the same shearing resistance. This is possibly due to full expansion of the apparatus, which would make points 2-7 invalid.

The depths of failure planes from the hole surface was inferred by measuring hole diameters before and after shearing. This depth was found to increase with applied normal stress, leveling off above stresses high enough to cause a structural breakdown of the plaster, and of a magnitude indicative that the apparatus may have reached full expansion. The shear planes under higher applied normal stresses showed a unique shallow saw-tooth or stair-step effect, but this was not pronounced at lower stress levels and may relate

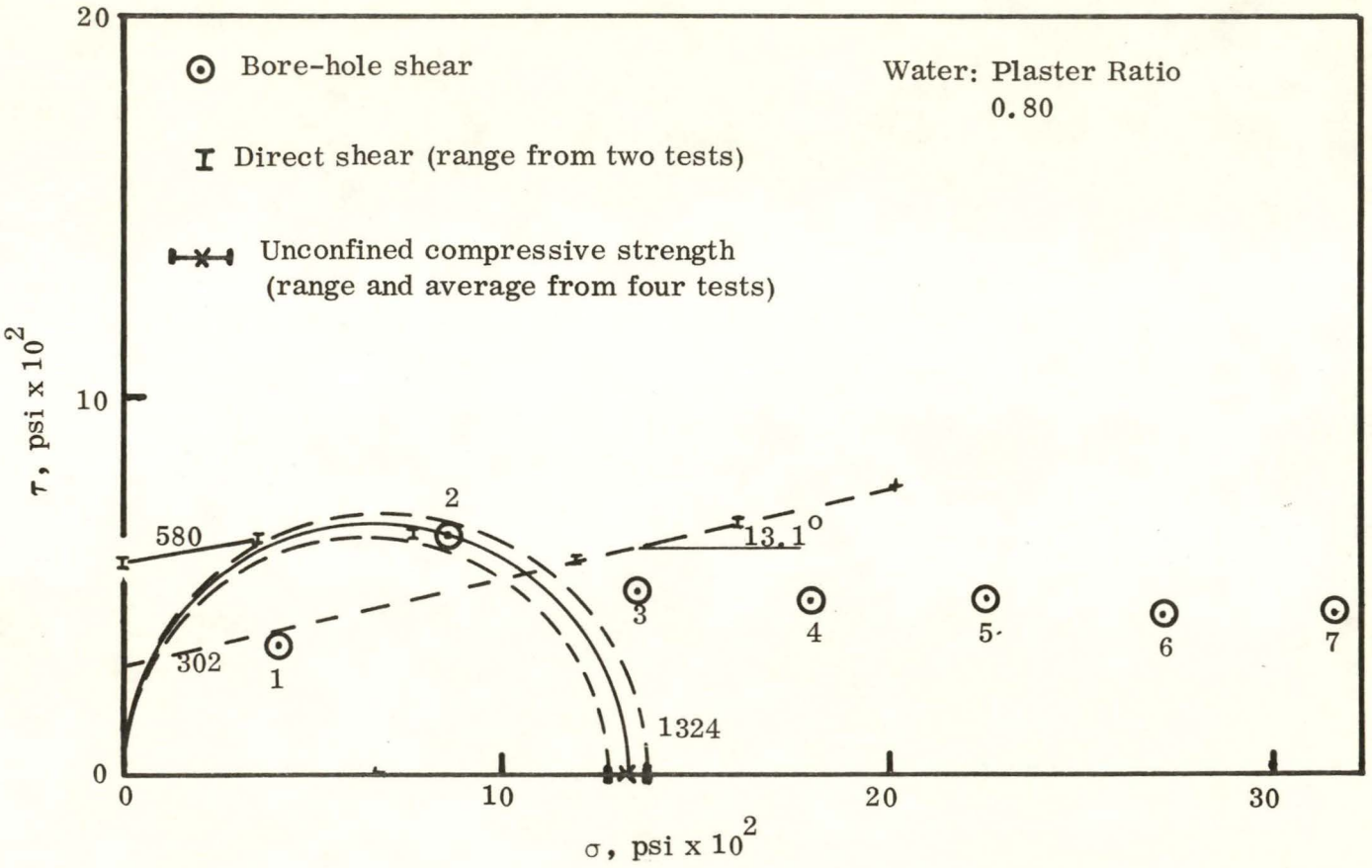
20
10
0
Bore-hole shear
Water: Plaster Ratio
0.80
Direct shear (range from two tests)
Unconfined compressive strength
(range and average from four tests)
τ, psi x 10^2
580
302
13.1°
1
2
3
4
5
6
7
1324
0
10
20
30
σ, psi x 10^2

Figure E2.

Table E1

Results of Direct Shear Tests on Plaster

Water: Plaster Ratio (by weight)		Unconfined Compressive Strength, q_u, psi	Cohesion c, psi	Remolded cohesion, psi	φ, °
0.70		1944	724	583	9.8
		1653	715	409	17.5
	Aver.	1798	720	496	13.6
0.80		1364	588	329	12.0
		1283	572	276	14.2
	Aver.	1324	580	302	13.1
0.90		987	481	145	15.4
		903	422	84	21.7
	Aver.	945	452	114	18.6
1.00		799	328	116	18.1
		767	383	0	26.7
	Aver.	783	356	58	22.4

to full expansion.

The results from plaster tests were encouraging insofar as the equipment was concerned, but testing was discontinued because plaster was a poor model for coal.

APPENDIX F

Tests on Neat Cement

Neat cement pastes were prepared by mixing Type I portland cement with varying amounts of water, the ratio of water weight to cement weight being referred to as the water-cement (w/c) ratio. Specimens were left in the molds eight hours, then extruded and allowed to air-dry. Submerged curing was found to increase strengths erratically and to too high a value to model coal.

Triaxial Tests

Typical Mohr circles from triaxial tests of neat cement are shown in Figure F1.

Table F1. Summary of triaxial tests on neat cement.

Water:cement ratio	Air curing time, days	φ_o	c, psi	No. of tests	q_u, psi
0.25	7	28.8	3072	3	10,376
0.25	14	31.6	2009	4	7146
0.30	7	35.1	1791	3	7015
0.30	14	28.1	2593	4	8381
0.35	7	24.3	2247	3	7121
0.35	14	26.0	2214	4	6450
0.40	7	33.5	1134	4	4013
0.40	14	27.0	1426	3	6004
0.45	7	22.7	1362	4	3992
0.45	14	17.8	1507	3	4018
0.50	7	8.8	1496	4	3349
0.50	14	7.3	1650	3	3625

Bore-Hole Shear

Data obtained from bore-hole shear (BHS) on essentially the same neat cement are shown in Figure F1 and Table F2. Since the sample sizes and hence curing differed, the bore-hole shear specimen was diamond-cored to obtain 0.5-inch diameter cores. The unconfined compressive strength of these cores was somewhat less, as shown by a dashed circle in Figure F1.

The bore-hole shear test did not measure cohesion, and the friction angles obtained were quite consistent but higher than those from triaxial tests. These are shown

Table F2. Summary of bore-hole shear and unconfined compression tests on neat cement.

Water:cement ratio	Air curing time, days	φ_o	c psi	No. of Test points	q_u, psi
0.25	7	36.2	19	8	5745
0.25[a]	21	38.0	40	8	5398
0.30	7	37.8	51	8	5321
0.30[a]	21	37.6	126	8	4775
0.35	7	38.9	-32	8	4985
0.35[a]	33	37.0	196	4	3923
0.40	7	32.3	132	8	2772
0.40[a]	33	37.1	88	4	5181
0.45	7	34.5	34	8	2792
0.45[a]	33	34.7	302	4	2893
0.50	33	36.3	136	4	3904

[a]Samples in which the model bore hole was not pregrooved.

versus water-cement ratio in Figure F2. Also from the figure can be seen that the effects of longer curing of triaxial samples or of pre-grooving the bore-hole shear samples were negligible or inconsistent. In general the closest agreement between triaxial and bore-hole shear friction angle data is a low water-cement ratio. At higher w/c ratios the φ from triaxial tests decreased, suggestive of positive pore water pressures.

High pressure double direct shear tests were not conducted on neat cement because the measured cohesions were too high and would cause the center plate to fail in bearing before failure shearing stresses were attained in the cement.

The shear tests on neat cement confirmed satisfactory operation of both the triaxial and bore-hole shear apparatuses, prior to the tests on coal.

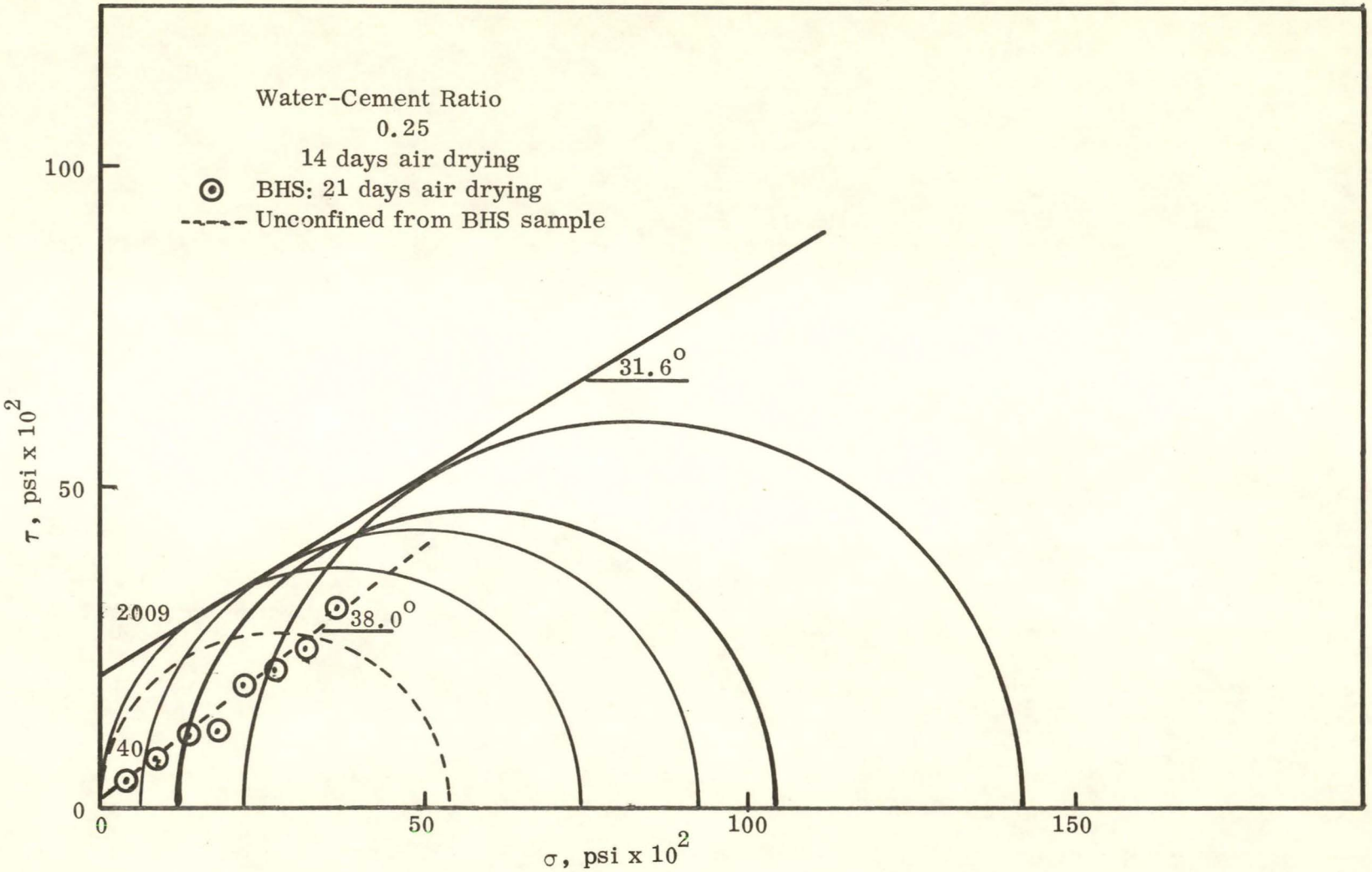

Figure F1. Representative BHS and triaxial data on neat cement.

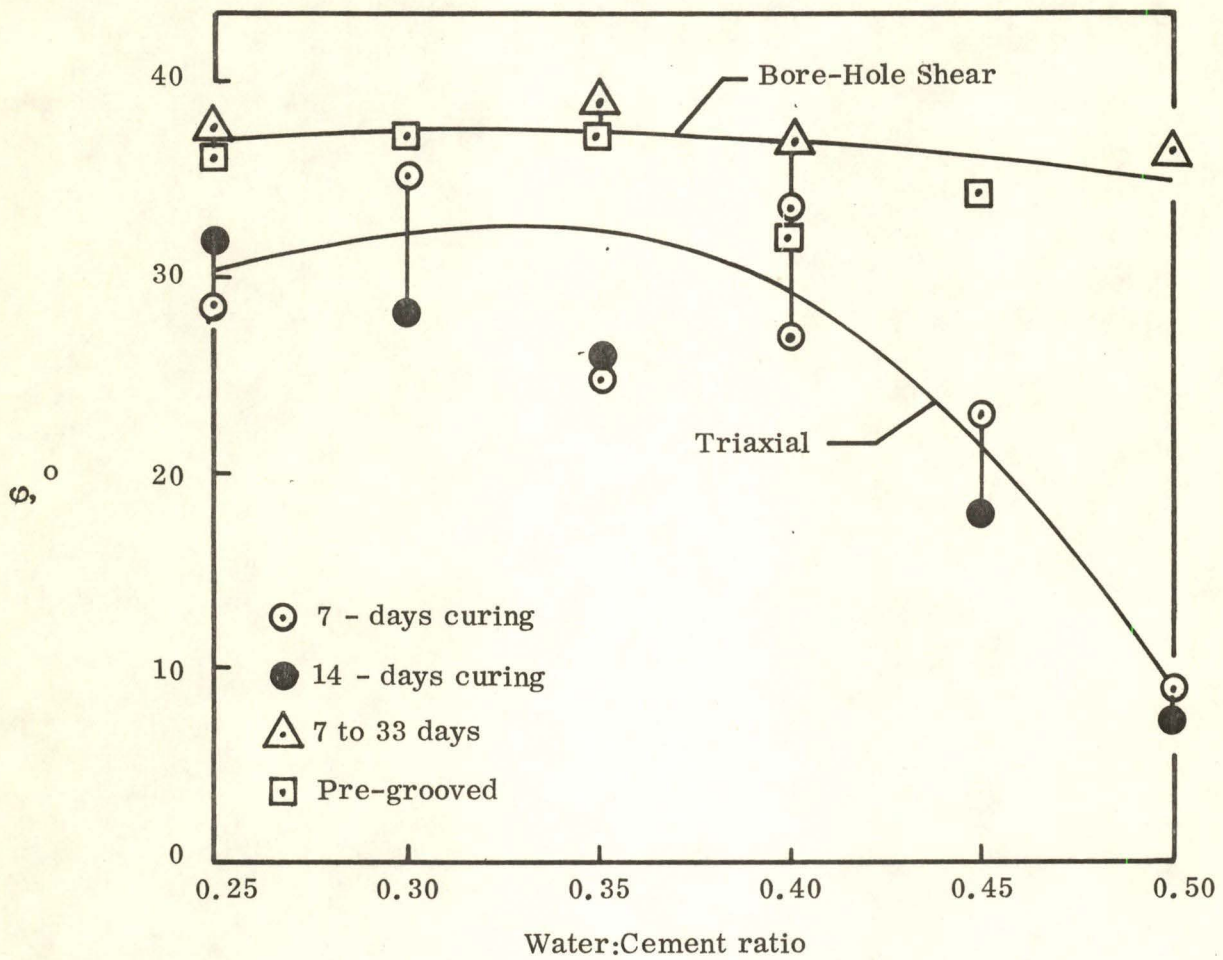

Figure F2. Friction angles from BHS and from triaxial tests.

Appendix G. Influence of Pre-Shear Techniques on Cohesion Measured by Bore-Hole Shear

Sample	φ	σ_i	τ_i	$\sigma_i \tan \varphi$	c_i
Series B, Parallel to Bedding:					
Q	35.0°	443 psi	378 psi	310 psi	68 psi
T	37.1	443	330	335	-5
U	34.8	443	402	308	94
C1	33.2	443	402	290	112
D1	33.0	443	390	288	102
E1	33.8	443	342	297	45
F1	36.9	443	294	333	-37
G1	35.2	443	402	313	89
Av.	34.9				58.5
Perpendicular to Bedding:					
S	30.7	938	1180	557	623
Z	36.2	443	402	324	78
A1	33.1	443	354	289	65
B1	30.2	443	366	258	108
H1	34.4	443	342	303	39
I1	35.5	443	550	316	234
J1	36.2	443	354	324	30
Av.	33.8				168
Series C1, Parallel					
R1	33.1	443	630	289	341
S1	32.6	443	463	283	180
Av.	32.8				260
Perpendicular					
K1	37.0	443	451	334	117
L1	35.5	443	523	316	207
Av.	36.2				162
Series C2, Parallel					
T1	32.5	443	439	282	157
W1	38.4	443	487	351	136
Av.	35.4				146

Sample		φ	σ_i	τ_i	$\sigma_i \tan \varphi$	c_i
Perpendicular						
M1		31.5[a]	443	619	271	347
N1		35.1	443	499	311	188
Q1		35.2	443	547	316	231
	Av.	33.9				255
Series C3, Parallel						
U1		34.6	443	571	306	265
V1		35.2	443	595	313	282
	Av.	34.9				274
Perpendicular						
O1		38.9	443	499	357	142
P1		38.0	443	583	346	233
	Av.	38.4				190
Series D1, Parallel						
D2		37.4	443	535	339	196
E2		39.7	443	667	368	299
	Av.	38.6				248
Perpendicular						
X1		40.9	443	631	384	247
Y1		34.3	443	499	302	197
	Av.	37.6				222
Series D2, Parallel						
F2		38.7	443	750	355	395
G2		36.2	443	607	324	283
	Av.	37.4				339
Perpendicular						
A2		31.7	443	559	274	285
Z1		36.5	443	619	328	291
	Av.	34.1				288

[a] Relaxation test data; sample damaged during application of normal stress.

Sample	φ	σ_i	τ_i	$\sigma_i \tan \varphi$	c_i
Series D3, Parallel					
H2	34.7	443	523	307	216
I2	34.3	443	631	302	329
Av.	34.5				272
Perpendicular					
C2	36.1	443	547	323	224
B2	36.3	443	571	323	248
Av.	36.2				236

U.S. DEPARTMENT OF LABOR MSHA
00024312